

THE PENNSYLVANIA STATE UNIVERSITY
SCHREYER HONORS COLLEGE

DEPARTMENT OF GEOSCIENCES

Carbon, Nitrogen and Manganese in Shale Soil Profiles along a Climate Gradient

NINA BINGHAM
SPRING 2013

A thesis
submitted in partial fulfillment
of the requirements
for a baccalaureate degree in Geosciences
with honors in Geosciences

Reviewed and approved* by the following:

Susan Brantley
Distinguished Professor of Geosciences
Thesis Supervisor

Maureen Feineman
Assistant Professor of Geosciences
Honors Adviser

* Signatures are on file in the Schreyer Honors College.

ABSTRACT

Addition profiles show a net enrichment of an element, j , at the surface compared to the parent material. The excess concentration of the element is coming from an outside source, is deposited on the surface and then subsequently incorporated into the soil profile through a variety of processes. The shape of these profiles can give clues to what processes are occurring in the soil and have the largest effect on the element, j . Carbon and nitrogen are elements associated with organic matter and can attribute most of their deposition to the decay of plant litter on the surface. Manganese is often used in metal refineries and input into the atmosphere and eventually “rained out” onto the soil. We analyzed these three element’s concentrations in soils at samples sites which make up a climosequence down the east coast of the United States with end members in Wales and Puerto Rico. C and N display addition profiles at every sample site. Mn only displays addition profiles in Pennsylvania and Virginia. We also determined the total concentration of C, N and Mn at each sample site with respect to the parent material for the soil and with account for soil strain. These values were compared against the mean annual temperature for each site. We saw a general increase in enrichment until $\sim 11^{\circ}\text{C}$ (after the Virginia site) and then a general decrease in enrichment until eventually every element studied was depleted at our end member in Puerto Rico. Pennsylvania has anomalously small concentrations of C and N compared to all other sample sites. We then fit our concentration profiles with a previously described diffusion based soil mixing model to determine what soil processes were acting on the soils in our transect. We discovered that soil mixing does not trend with mean annual temperature. We knew that the model greatly underestimated the input rates of C and N because of the model’s simplicity. The most realistic values for C and N input were determined for the Wales profile because Wales had high annual precipitation and low mean annual temperature which retards soil organic matter decomposition. Additionally, we realized that organic matter decomposition, which was not

included in the model, plays an integral part in the more southern sample sites. This is especially true at the warmest sample site, Puerto Rico. There, the C and N inputs were large yet the profile was still depleted of C and N. The model did a good job at explaining accurately the transport and storage of Mn in the soil assuming Mn is relatively immobile. This means that the major process affecting the distribution of Mn in the soil is soil mixing. Also, Mn increases showed no trend with climate. A more complete (more processes incorporated) is necessary to better quantify soil processes associated with C and N storage and subsequently explain trends in SOM storage with temperature.

TABLE OF CONTENTS

Section Title	Page Number
List of Figures	iv
List of Tables	v
Acknowledgements	vi
Introduction	1
Methods	3
Results	10
Discussion	19
Conclusion	33
Appendix	35
Works Cited	42
CV	44

LIST OF FIGURES

Figure Number: Name	Page Number
Figure 1a: Spatial map of the sampling locations	4
Figure 1b: Latitude of sample sites vs. MAT of the sample locations	4
Figure 2: C concentration vs. profile depth for each sample site	11
Figure 3: N concentration vs. profile depth for each sample site	12
Figure 4: Mn concentration vs. profile depth for each sample site	13
Figure 5: C τ values vs. profile depth for each sample site	14
Figure 6: N values vs. profile depth for each sample site	15
Figure 7: Mn values vs. profile depth for each sample site	16
Figure 8: Mj for C, N and Mn at each sample site vs. MAT	17
Figure 9: mj for C, N and Mn at each sample site vs. MAT	18
Figure 10: C/N ratio vs. profile depth for each sample site	19
Figure 11: Model fits to C & N concentration profiles at Wales	22
Figure 12: Model fits to C, N & Mn concentration profiles at PA	23
Figure 13: Model fits to C, N & Mn concentration profiles at VA	24
Figure 14: Model fits to C & N concentration profiles at Tennessee	25
Figure 15: Model fits to C & N concentration profiles at Alabama	26
Figure 16: Model fits to C & N concentration profiles at PR ($D_{eff}=1.9 \text{ cm}^2\text{yr}^{-1}$)	27
Figure 17: Model fits to C & N concentration profiles at PR ($D_{eff}=3.9 \text{ cm}^2\text{yr}^{-1}$)	28
Figure 18: D_{eff} values from model fits for each site vs. MAT	29

Figure 19: C & N input rates from model fits for each site vs. MAT	30
Figure 20: C, N & Mn concentration profiles for Wales	35
Figure 21: C, N & Mn concentration profiles for Pennsylvania and soil horizon names	36
Figure 22: C, N & Mn concentration profiles for Virginia and soil horizon names	37
Figure 23: C, N & Mn concentration profiles for Tennessee and soil horizon names (abbreviated profile)	38
Figure 24: Full C, N & Mn concentration profiles for Tennessee	39
Figure 25: C, N & Mn concentration profiles for Alabama	40
Figure 26: Full C, N & Mn concentration profiles for Puerto Rico	41

LIST OF TABLES

Table Number: Name	Page Number
Table 1: Sample site descriptions	5

ACKNOWLEDGEMENTS

I would like to thank my friends and family for obligingly listening to me explain addition profiles and mathematical models even when you didn't have any idea what I was saying. I would also like to thank Megan Carter-Thomas for her unending support and intellectual discussions about manganese. I would like to acknowledge Ashlee Dere; without her I could not have done any of this. And finally I would like to thank my advisers Sue Brantley and Maureen Feineman, who provided guidance and had much tolerance along the way. Thank you all.

1. Introduction

Soils are dynamic; a variety of physical, chemical and biological processes act upon them over varying timescales. Due to the changes occurring in soils, it is of great importance to track how these changes affect nutrients, toxins and trace metals in soils. Some elements form addition profiles in soil, meaning an element increases in concentration from the basal layer of soil to the surface (Yaalon and Ganor 1973; Brantley and Lebedeva 2011). These additions are indicators of concentrations in the soils that are in excess of what is expected based on the composition of the parent rock (protolith). This can be beneficial for ecosystems in terms of essential elements for plant growth and soil productivity: carbon and nitrogen for example. Or excessive concentrations of certain elements in the soil can be negative in the case of toxin build ups, like manganese.

Mn is toxic to humans in varied quantities; it can cause brain degeneration to animals when exposed to high levels of manganese (U.S E.P.A. 2003). During the most recent century, Mn was used heavily in making steel, iron and ferromanganese alloys. The Mn is released into the air from factory emissions and accumulates on the earths soils during precipitation events (Herndon et al. 2011). Carbon and nitrogen owe much of their input to soils by natural cycles which include surficial input from leaf litter and fixation by plants and microorganisms at depth. Soil organic matter (SOM), which is predominantly made up of the elements C & N, has been linked with temperature changes (Jobbagy and Jackson 2000; Davidson and Janssens 2006).

There are many concerns with how global warming will affect our environment, including concerns for how the soils we live on and rely upon for food will change. These changes in soils may reflect on the storage or transport of many elements and compounds held in the soil.

Determination of how C, N and Mn concentrations change in a warming climate could provide important information for better management of agricultural practices, carbon sequestration studies and prevention of toxicity events. In this thesis I target a climosequence: a set of soil sample sites along a transect of locations that vary with respect to mean annual temperature,

MAT, and mean annual precipitation, MAP. This climosequence is used in this study as a proxy for investigating the effect of global warming on soil processes. Importantly, the climosequence used in this study is underlain by similar parent material: organic-poor shale. Shale, compared to other rocks is relatively limited in its mineralogical make-up, thus providing a simple parent material (Dere et al. 2013).

Models provide another method of analyzing field data and if properly implemented can add to our understanding of the processes observed in the soil. Due to the importance of soil organic matter dynamics in agricultural practices, the leading SOM models are quite extensive. Today's models for soil organic matter incorporate variables that include meteorological data, plant material information, soil texture, atmospheric and soil nitrogen input and soil chemistry data. The most notable of large SOM models are CENTURY and DAYCENT, which run on either month or day timescale (Parton et al. 1998; Parton et al. 1996). These models produce highly accurate descriptions for the typical grassland agricultural system and have the ability to provide model descriptions of forest landscapes; however, the complexity of the model prevents the application to smaller scale studies with limited data.

The task of creating a simpler model without forgoing accuracy has also been explored in detail over the years. Modeling relatively immobile elements such as lead and in some cases manganese has been successful using simple advection-diffusion or just diffusive-like mixing models (Kaste et al. 2007; Drivas et al. 2011). Simpler models for SOM and specifically C and N have evolved over time through the pursuit of trends with carbon storage with temperature, soil texture and vegetation (Jobbagy and Jackson 2000; Davidson and Janssens 2006). Presently, models by Braakhekke (2011), Baisden et al (2002) and Elzein and Balesdent (1994) have all incorporated from three to five carbon pools as well as processes such as diffusion, advection and SOM decomposition to move carbon (and nitrogen) between pools throughout the entire profile and out of the profile. Each pool of SOM contains C, N or both and has a different rate of

decomposition. The models simulate the variety in soil organic matter residence times observed in natural environments: rapid turnover on a yearly scale, medium-slow turnover on a decadal scale, and finally an almost stable pool of carbon with a millennial scale turnover rate (Braakhekke et al. 2011; Baisden et al. 2002; Elzein and Balesdent 1995). Generally, the rapidly decomposing pool is most often associated with surficial carbon pools while the stable C pool is associated with deeper depths of C stored in the mineral structure. For this study, we want to utilize the simplest model possible to fit to the C, N and Mn concentration profiles we observed from our data. A simple model will allow us to examine one process (soil mixing) and if this process provides an adequate explanation for the observed profiles or if there is a need for other parameters or soil processes. In this study we will apply the diffusive-mixing model as described by Drivas et al (2011) to our Mn, C and N concentration data to help explain trends seen between total element concentrations in profiles and climate variables.

2. Methods

2.1 Sample locations and collection techniques

Soil samples were taken from six sites which form a climosequence over a 34° latitudinal spread; the temperatures range between 7.2 °C – 24 °C. There are four sites on the east coast of the United States -- Pennsylvania (PA), Virginia (VA), Tennessee (TN) and Alabama (AL) -- and a cold, wet end member in Wales (W) and a warm, wet end member in Puerto Rico (PR). Figure 1a shows a map of the sample locations for reference. Figure 1b shows latitude of the sample sites plotted against mean annual temperature (MAT) to better portray the climosequence.

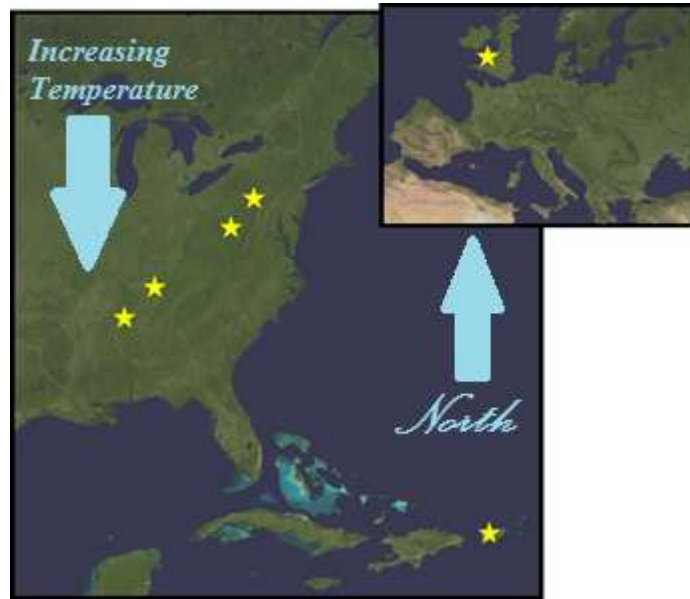


Figure 1a. Spatial map of sampling locations for the study.

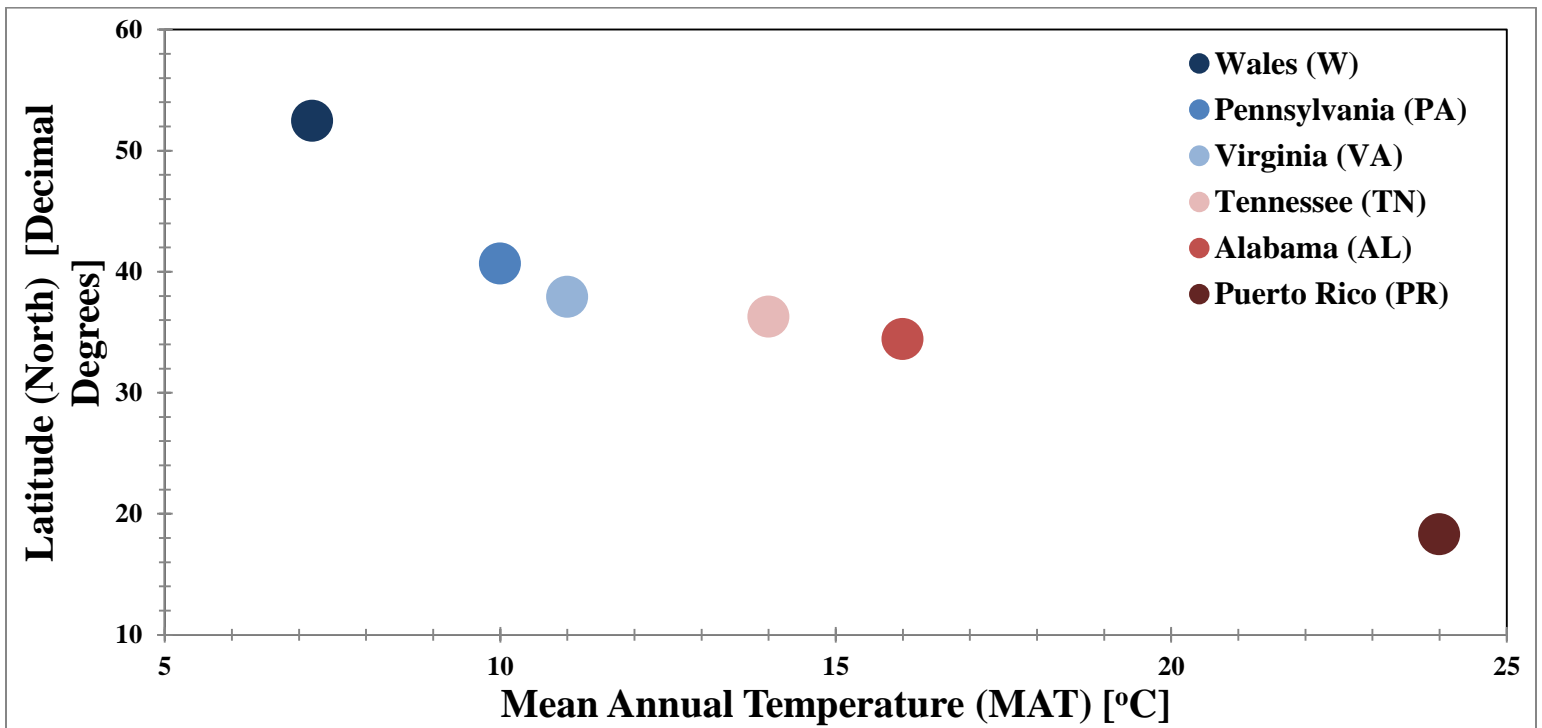


Figure 1b. Latitude in decimal degrees plotted against MAT in °C. All latitudes are north of the equator. Sample sites MAT increases as their latitudes decrease.

The sites were all chosen as ridgetop sites because these locations can be modeled as one dimensional water flow systems. All sites have similar underlying geology (iron-rich, organic

poor shale) and are located in relatively undisturbed forested areas (PA site has been cleared due to logging 2-3 times since the 1700's and PR has been fallow farming land for 40 years). Table 1 provides a detailed list of site information for each sample site (Dere et al. 2013)

Table 1. Soil sample site characteristics

Site	Latitude	Longitude	Elevation [m]	Relief [m]	Slope [o]	MAT [°C]	MAP [cm]	depth [cm]
Wales	N52° 28.416	W3° 41.575	417	87	0.29	7.2	250	35
Pennsylvania	N40° 39.931	W77° 54.297	297	40	0.1	10	107	28
Virginia	N37° 55.625	W79° 32.799	752	220	0.34	11	106	80
Tennessee	N36° 16.414	W83° 54.809	418	71	0.3	14	138	398
Alabama	N34° 25.375	W86° 12.400	241	43	0.35	16	136	220
Puerto Rico	N18 18.050	W66 54.401	366	25	0.16	24	234	613

Soil and rock samples were collected previous to this study as outlined in Dere et al. (2013). Soil samples were collected by hand augering to the depth of refusal, or the point at which a hand auger cannot be driver further (Dere et al. 2013). Soil samples were collected in ~10 cm intervals to refusal. Additionally, soil pits were dug at most of the sites and physical properties were described (Soil Survey Staff 1993). Figures 20-26 show the identified horizon names for most soil sample locations. In TN, AL and PR, hand augering was continued from the bottom of the soil pit until refusal. The profiles vary greatly in depth between 28 cm (PA) and 632 cm (PR).

Rock samples to be used as parent material for the overlying soils were collected from exposed outcrops near the ridges. Soil samples and rock fragment samples were taken from the

bottom of soil pits (if fragments were present). These outcrop locations were taken after careful stratigraphic consideration and their proximity to the sampling locations.

2.2 Sample Analyses

Bulk soil samples (all size fractions) were air-dried, crushed, and ground. After grinding, samples were split with a riffle soil splitter four times. Rock and soil samples were then completely ground by hand using a mortar and pestle to <149 microns (100 mesh). This bulk sample was then analyzed for all sites.

Major elements were measured by inductively coupled plasma atomic emission spectroscopy on a Perkin-Elmer Optima 5300DV Inductively Coupled Plasma-Atomic Emission Spectroscopy (ICP-AES) (Penn State Materials Characterization Lab (PSU-MCL), Senior Analyst Henry Gong). Following the process outlined by Medlin et al, (1969), samples were prepared for ICP-AES by fusing 100 mg of the ground sample with 1 g of lithium metaborate at 950 °C and then promptly dissolving the fused sample in a 5% nitric acid solution for 30 minutes (Medlin et al. 1969).

Total carbon and total nitrogen were measured on a CE Instruments Elemental Analyzer EA 1110 with a thermal conductivity detector (Soil Research Cluster Lab PSU). Between 13-18 mg of samples were weighed and loaded into tin vials for combustion using a combination of two precision scales. One reference sample was run twice before our samples and every 10 samples a duplicate was run to ensure reproducibility of the data.

2.3 Preliminary Data Processing

Soil bulk density, ρ_b [g cm^{-3}] was used in many of the preliminary data calculations; our bulk densities were calculated using the equation outlined in Dere et al. (2013) and reproduced below as equation 1. Equation 1 shows that bulk density can be accurately estimated for any sample from any depth using a value for the maximum reasonable bulk density, b [g cm^{-3}], a surface bulk

density, ρ_b^o [g cm⁻³], a fit parameter related to the slope, K, and the depth of the soil sample, z [cm] (Dere et al. 2013)

$$\rho_b = \rho_b^o + \frac{(\rho_b^{max} - \rho_b^o)Kz}{1-Kz} \quad (1).$$

The mass transfer coefficient, τ [unitless], is used to show relative addition or depletion of an element with respect to an immobile element after normalization with respect to the concentration of an immobile element in the parent material (Brimhall and Dietrich 1987; Anderson et al. 2002) Equation 2 defines τ where $C_{j,w}$ [wt. %] is the concentration of mobile element j in the weathered sample, $C_{j,p}$ [wt. %] is the concentration of j in the parent material, $C_{i,w}$ [wt. %] is the concentration of immobile element, i, in the weathered sample and $C_{i,p}$ [wt. %] is the immobile element concentration in the parent material

$$\tau = \frac{C_{j,w}C_{i,p}}{C_{j,p}C_{i,w}} - 1 \quad (2).$$

The elemental composition of parent material was determined by averaging element concentrations from the collected rock samples. The immobile element used for τ calculations for soils from W, PA, TN, AL and PR was Zr. However, the soil from Virginia exhibited a Zr concentration 3-5x larger than the concentration in the samples used for VA parent material. Thus, we could not use Zr as the immobile element at this site. Dere et al. (2013) argued that the sandstone stratigraphically above the shale is the source of the excess Zr, enriching the soil formed during its weathering. At the site now, the sandstone has been completely weathered away, but has left residual Zr in the shale soil (Dere et al. 2013). Thus, here, we followed Dere et al. (2013) and used the Ti concentration for the VA soil after correcting for Ti losses. Equation 3 describes the correction we used for the titanium concentration:

$$C_{Ti,corrected} = C_{Ti,actual} + \left(\tau_{Zr,Ti}^{TN} + C_{Ti,actual} \right) \quad (3).$$

($C_{Ti,corrected}$ [wt. %]) used in the τ calculations for Virginia as described by Dere et al (2013) and Jin et al. (2010). It is assumed that Ti in VA is lost in similar proportions to the Ti in TN at the same depth scale (Dere et al. 2013; Jin et al. 2010)

Calculation of total C, N or Mn in a profile was also completed to assess integrated concentrations for those elements. Two methods were used. The first is a simple summation of concentrations at each sampling interval to calculate M_j [g cm^{-2}] as shown in equation 4 (Brimhall and Dietrich 1987):

$$M_j = \sum C_j \rho_w dz \quad (4).$$

Here, $C_{j,w}$ [wt. %], is the concentration of element j, ρ_w [g cm^{-3}], is the bulk density of the soil at the depth z, and dz [cm] is the depth interval. The second method integrates τ values which have been corrected for soil strain over depth, producing net additions or depletions of an element with respect to the parent material (Brimhall and Dietrich 1987; Anderson et al. 2002; Brantley and Lebedeva 2011). The integrated mass outflux or influx, m_j [g cm^{-2}] is shown in equation 5:

$$m_j = C_{j,p} \rho_p \int_0^L \frac{\tau_j(z)}{\varepsilon(z)+1} dz \quad (5).$$

Although this is written as an integral, we calculated m_j by a summation of the values for each sampled depth interval. Here ρ_p is the density of the parent material, this is assumed to be a constant 2.64 [g cm^{-3}] which is an average for shales (Jin et al. 2010), L [cm] is the maximum depth of the profile, dz [cm] is the sample interval, $\tau_j(z)$ [unitless] is tau for element j at depth z and ε [unitless] is the soil strain for the soil interval. Soil strain is calculated using the equation originally derived by Brimhall and Dietrich (1987)

$$\varepsilon_i = \frac{\rho_p C_{i,p}}{\rho_w C_{i,w}} - 1 \quad (6).$$

2.4 Drivas et al. (2011) Model

Soil mixing via bioturbation, freeze/thaw, root-wedging, etc. can be most simply described by Brownian motion: a random diffusive motion of particles. Drivas et al. (2011) described the most basic model incorporating this process, the classic 1-D diffusive mixing equation as described by equation 7 (Drivas et al. 2011):

$$\frac{\partial C_j}{\partial t} = \mathbf{Deff} \frac{\partial^2 C_j}{\partial z^2} \quad (7).$$

The equation was solved analytically by Drivas et al. (2011) assuming steady-state; i.e., the concentration of elements, j , no longer changes in time. The variables z and t are soil depth [cm] and time [years] respectively. C_j is the concentration of the element at any depth interval [gcm^{-3}]. $Deff$ is the diffusive mixing coefficient; which describes the magnitude of soil mixing occurring per year [$\text{cm}^2\text{yr}^{-1}$]. Surficial deposition of element C_j (simulating leaf litter input for C and N or atmospheric deposition of Mn-sorbed particles) provides the only source of input for element C_j . Equation 7 was solved with two different assumptions with respect to surficial input: either a continuous surface deposition or a one time, extended interval of surface deposition of the element.

It is well known that carbon and nitrogen are constantly deposited to the surficial horizons of a soil profile via litter decomposition and root inputs, thus a continual surface input was used here to apply the Drivas et al. model for those elements. The steady-state solution for equation (7) from Drivas et al. for the assumption of a continuous surficial input is described as (Drivas et al. 2011):

$$C_s(z, t) = \frac{2Q}{Deff} \left[\sqrt{\frac{(Deff)(t)}{\pi}} \exp\left(\frac{-z^2}{4(Deff)(t)}\right) - \frac{z}{2} \operatorname{erfc}\left(\frac{z}{2\sqrt{(Deff)(t)}}\right) \right] \quad (8).$$

In equation 8, Q is the continuous surface deposition rate of element j per unit area [$\text{gyr}^{-1}\text{cm}^{-2}$], \exp is the exponential function and erfc is the complementary error function.

In contrast to C and N, Mn is deposited mainly via atmospheric deposition. For example, one researcher has concluded that most Mn in the northeast was deposited in soils as Mn sorbed to

dust (Herndon et al. 2011b). Accordingly, much of the Mn deposition in the eastern US to soils occurred over a period of ~70 years during the last century until the Clean Air Act significantly cut emissions (Herndon and Brantley 2011a). To represent this period of deposition, the model was solved with a timed deposition of 70 years during a 100 year run. Equation 9 represents the steady-state solution for this model as presented originally by Drivas et al. (2011):

$$C_s(z, t) = \frac{Qz}{Def f} \left[\sqrt{\frac{\exp(s_L^2)}{\sqrt{\pi}s_L} + \operatorname{erf}(s_L) - \left(\frac{\exp(-s_U^2)}{\sqrt{\pi}s_U} \right) - \operatorname{erf}(s_U)} \right],$$

here, the following terms are defined:

$$s_L = \frac{z}{2} \sqrt{(Def f)(t)} \quad s_U = \frac{z}{2} \sqrt{(Def f)(t - T)} \quad (9).$$

All other terms are defined previously; however, it should be noted that t is the total time for the model run and T is the time of deposition and Q is the surface deposition during the time T (Drivas et al. 2011).

3. Results

3.1 Concentration versus depth profiles

It is first prudent to gain knowledge of how the concentration profiles of C, N and Mn change with depth in order to gain insight into where the majority of the element is being stored in the soil profile. It is also necessary for the Drivas et al. (2011) model to have concentration profiles versus depth. The profiles presented were cropped at 200 cm if necessary to show the concentration profile dynamics which occur in the top 200 cm of soil. Full concentration profiles can be seen in figures 20-26 in the Appendix.

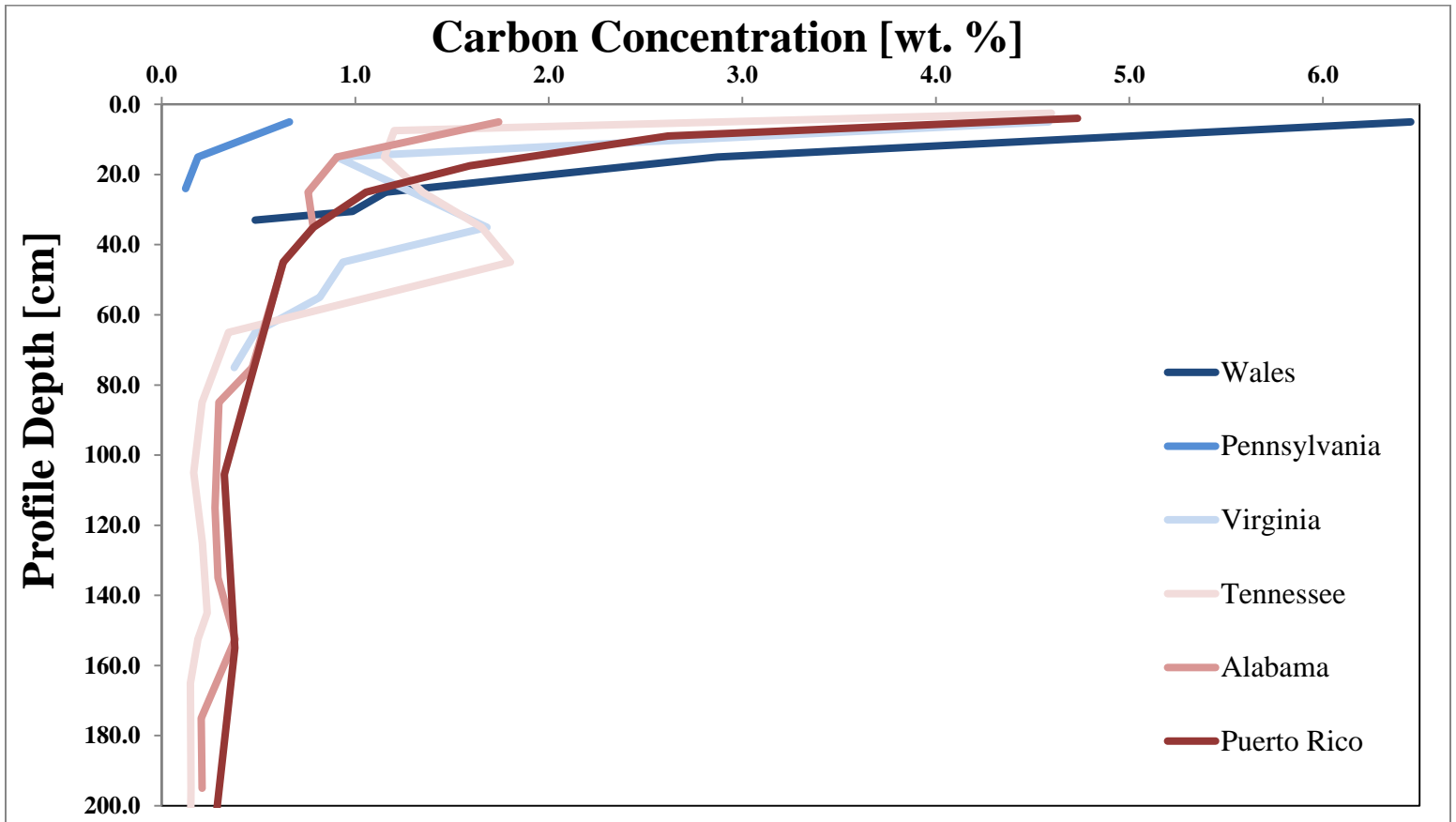


Figure 2. Carbon concentration versus depth for each sample site. The concentration profiles are plotted against profile depth to 200 cm. Only Puerto Rico and Tennessee extend further than 200 cm; however, the change in their concentrations at deeper depths is minimal compared to the concentrations at 200 cm. The colors change from ; dark blue (coolest climate, Wales) to dark red (warmest climate, Puerto Rico).

Wales has the most C on the surface, followed by Puerto Rico, Tennessee, Virginia, Alabama and finally Pennsylvania; with the least amount of C at the surface. In every soil, the carbon and nitrogen concentrations generally decreased with depth (Figures 2 and 3). However, small increases in carbon were observed between 20 cm and 60 cm for Virginia (VA) and Tennessee (TN). This “bump” at depth was not seen in Wales (W), Pennsylvania (PA), Alabama (AL) nor Puerto Rico (PR). The apex of the “bump” moves downward in depth with decreasing latitude (i.e., increasing MAT) between VA and TN.

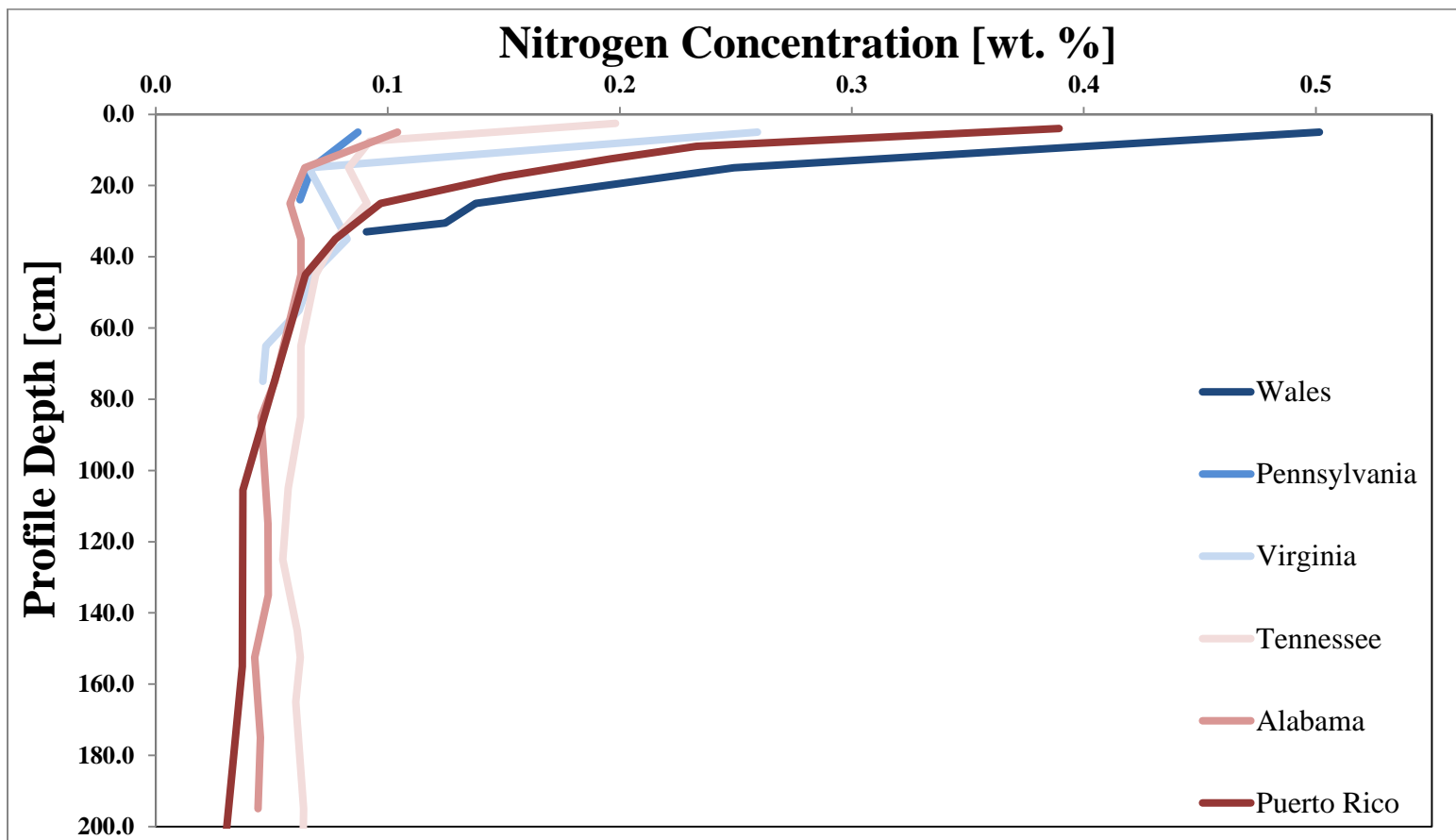


Figure 3. Nitrogen concentration versus profile depth for each sample site. Once again the sample locations are color coded for temperature (dark blue=coolest to dark red=hottest). The concentration profiles are also displayed against profile depth to 200 cm. Only Puerto Rico and Tennessee extend further than 200 cm; however, the change in their concentrations is minimal from the concentrations at 200 cm.

The “bumps” which were observed in the carbon profiles for VA and TN are also seen in the nitrogen profiles for VA and TN on a smaller scale (the increase at depth is less dramatic than in the C profile). At the surface, Wales has the highest concentration of nitrogen, and then followed by Puerto Rico, Tennessee, Virginia, Alabama and then Pennsylvania. Overall, these profiles mimic the carbon profile shapes; however, the concentration is approximately one order of magnitude smaller.

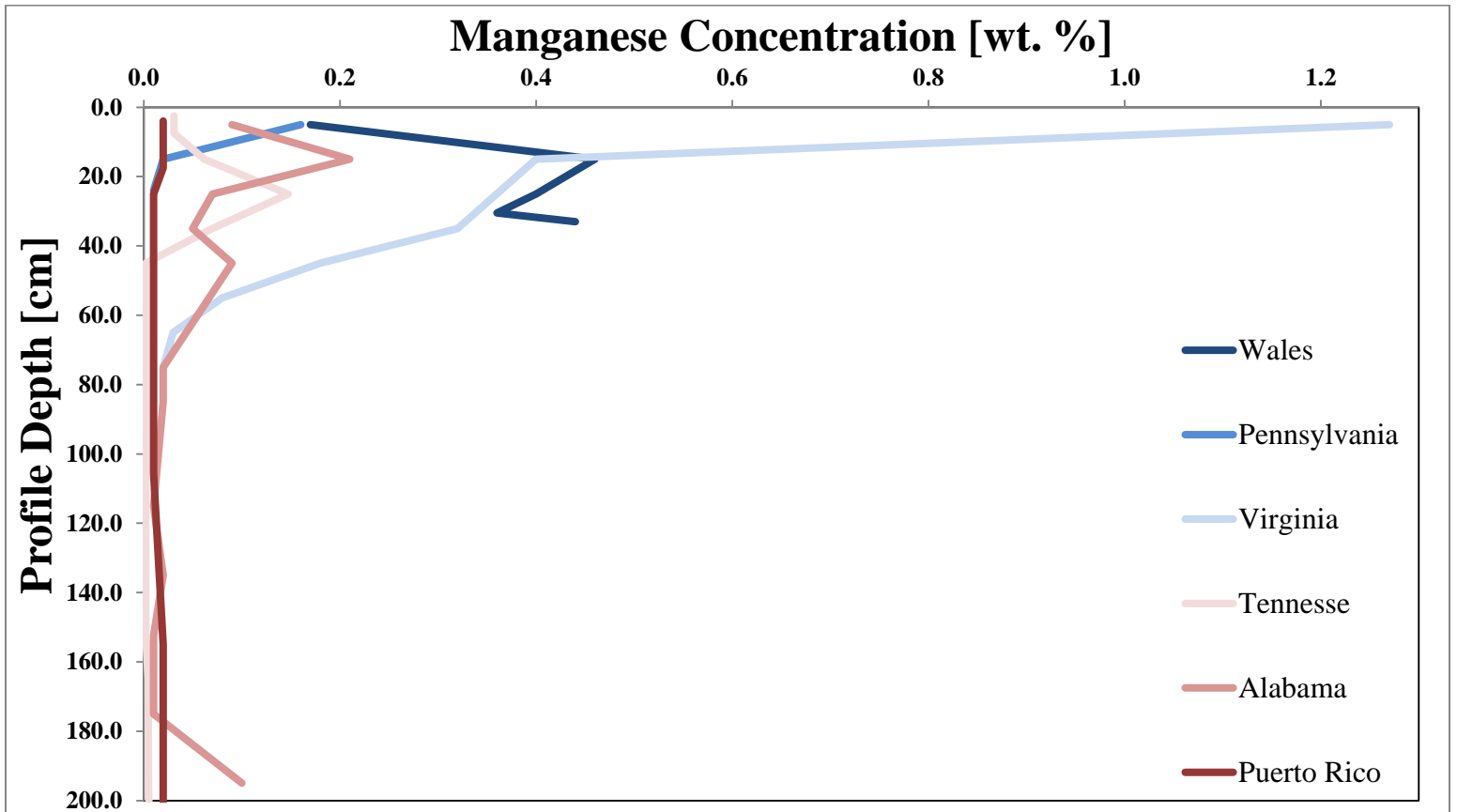


Figure 4. Manganese concentration versus profile depth. The samples sites are similarly color coded for increasing MAT, dark blue-coolest climate to dark red-warmest climate. The concentration profiles are displayed against profile depth to 200 cm. Only Puerto Rico and Tennessee extend further than 200 cm; however, the change in their concentrations is minimal from the concentrations at 200 cm.

Unless enriched from the parent material, generally manganese is not present in large quantities in the soils shown in figure 4. Virginia has high Mn concentrations compared to all other sites: just over 1.2 weight percent compared to all other values which were less than 0.2 weight percent. In Wales, the profile shape is similar to the shape of the Tennessee and Alabama profiles with increases; i.e. concentrations increase at depth (around 20-30 cm). Pennsylvania shows a small enrichment towards the surface.

3.2 Tau Plots

The Drivas et al. model works only for profiles which show net enrichment at the surface; true addition profiles. The mass transfer coefficient, τ , allows us to check the sampled profiles.

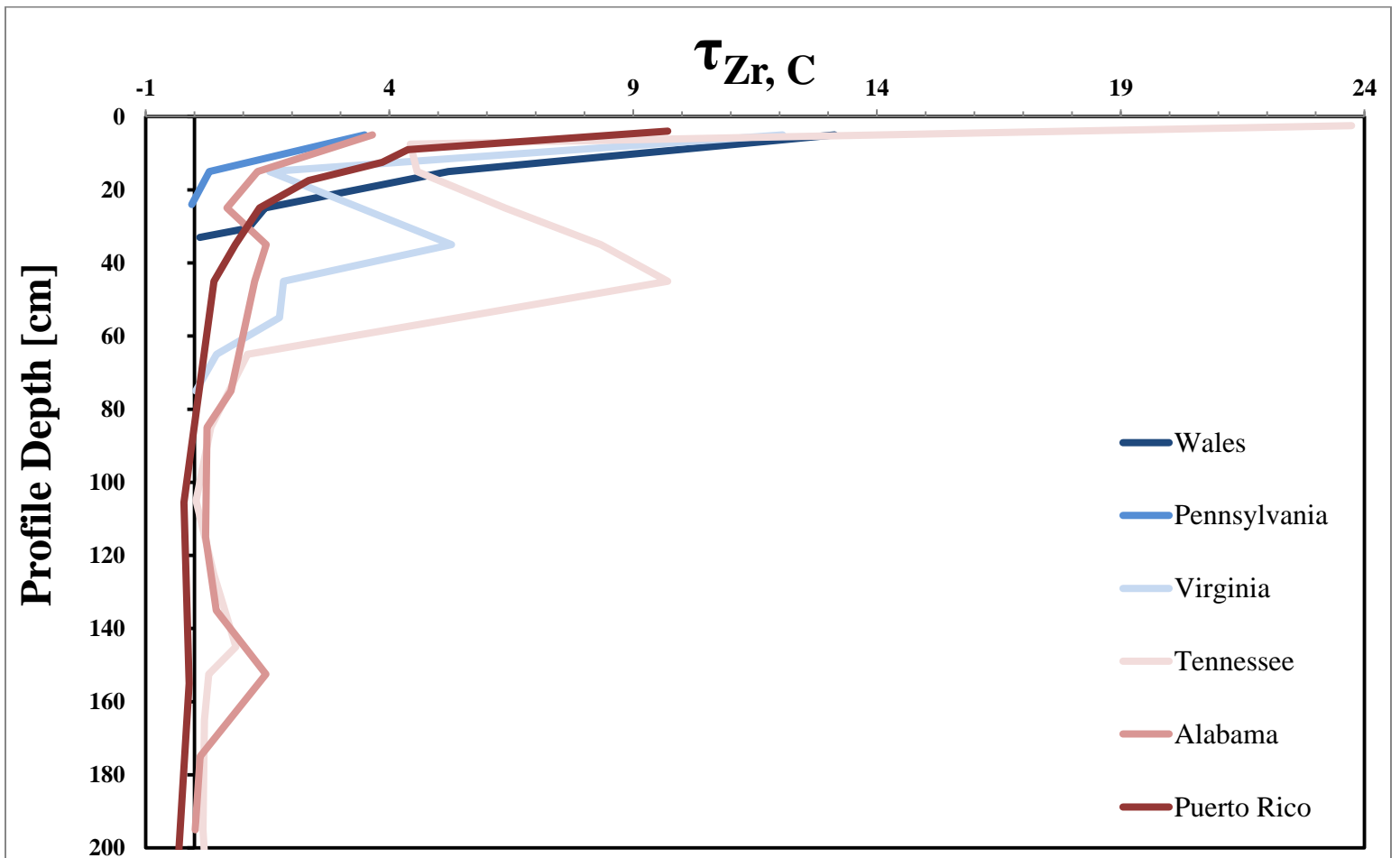


Figure 2. Mass Transfer Coefficient for carbon at all sites plotted versus depth. Parent material was assumed to equal the C concentration of the deepest soil sample for the full profile or an average of the 2 deepest soil samples' C concentration for each full profile. Wales, Virginia, Tennessee, Alabama and Puerto Rico used an average of the two deepest soil sample C concentrations. Pennsylvania used only the bottommost soil sample C concentration because the profile was so shallow. Zirconium is the immobile element for Wales, PA, TN, AL and PR sites. A corrected titanium concentration was used for the immobile element for VA.

All of the locations show addition profiles for carbon. An increase in carbon between 20 and 60 cm is once again visible in the VA and TN τ profiles. Puerto Rico appears to be slightly depleted below 100 cm. Tennessee shows the most surficial enrichment ($\tau=23.74$ for depth 0-1 cm) and Pennsylvania shows the least surficial enrichment ($\tau=3.49$ for depth 0-10 cm). It is interesting to note that Wales, which had the highest weight % for carbon at the surface, is second to Tennessee when looking τ values.

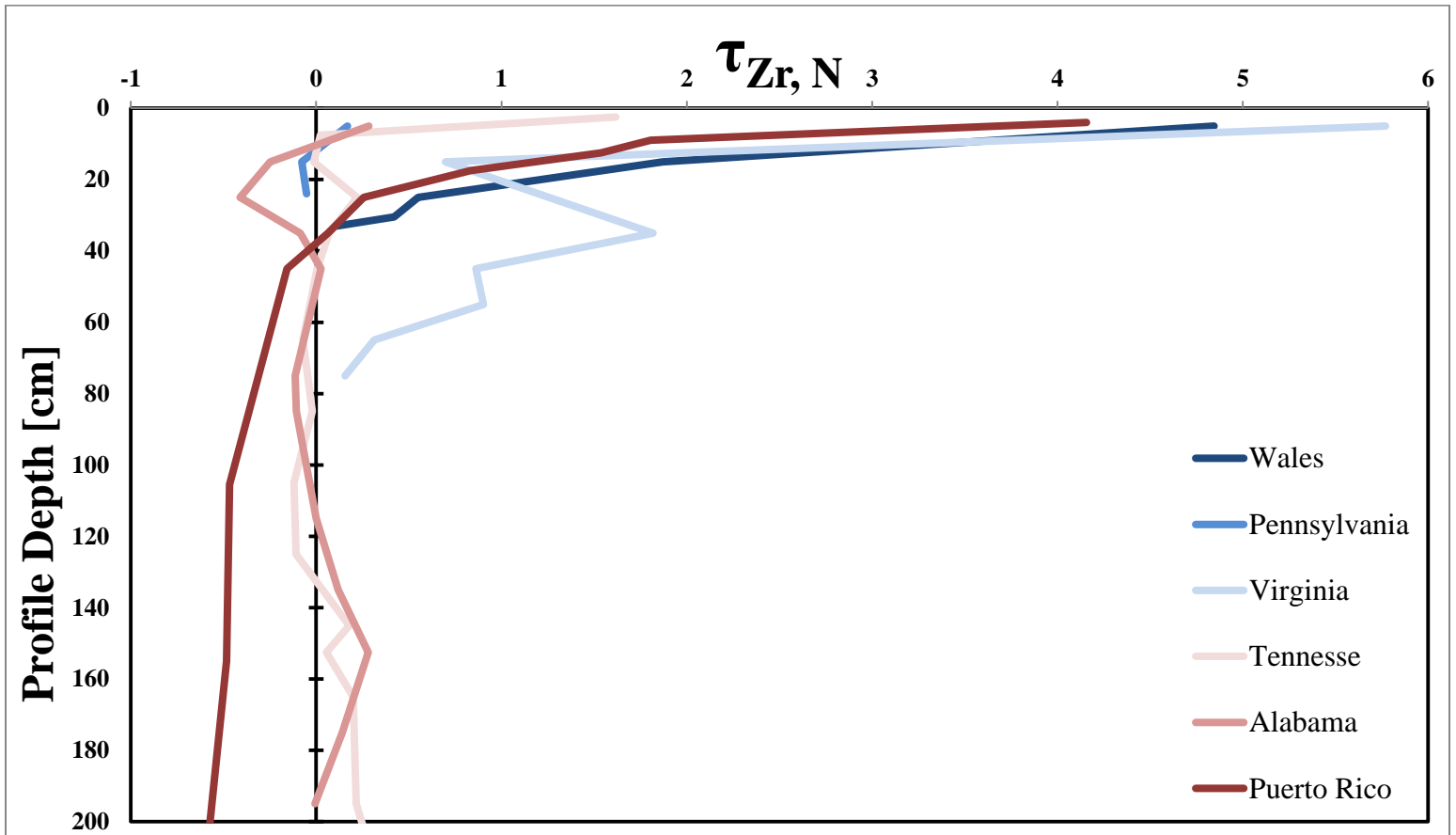


Figure 3. Mass transfer coefficient, τ , for nitrogen plotted versus depth at every site. Parent materials for all elements are exactly the same for the C τ plot (figure 5). Zirconium is the immobile element for Wales, PA, TN, AL and PR sites. A corrected titanium concentration was used for the immobile element for VA.

All sites are enriched at the surface with nitrogen; however, Alabama shows depletion just below the surface around 10 cm and then hovers around 0 throughout the rest of the profile. Tennessee returns to 0 net enrichment or depletions and also hovers around 0 to its basal layer of soil. It should be noted that TN does show a small increase in N around the area (20-30 cm) that the C and N increase was seen in TN when comparing weight percent's against profile depth (figures 2 and 3). The nitrogen profile shape for Virginia is similar to the carbon profile for Virginia; the "bump" in C around 40 cm is replicated in the N profile at 40 cm as well. Puerto Rico becomes depleted at 40 cm and stays depleted with depth. Wales is enriched at all depths. Pennsylvania is enriched to depths of 15 cm, where N becomes depleted at all deeper depths.

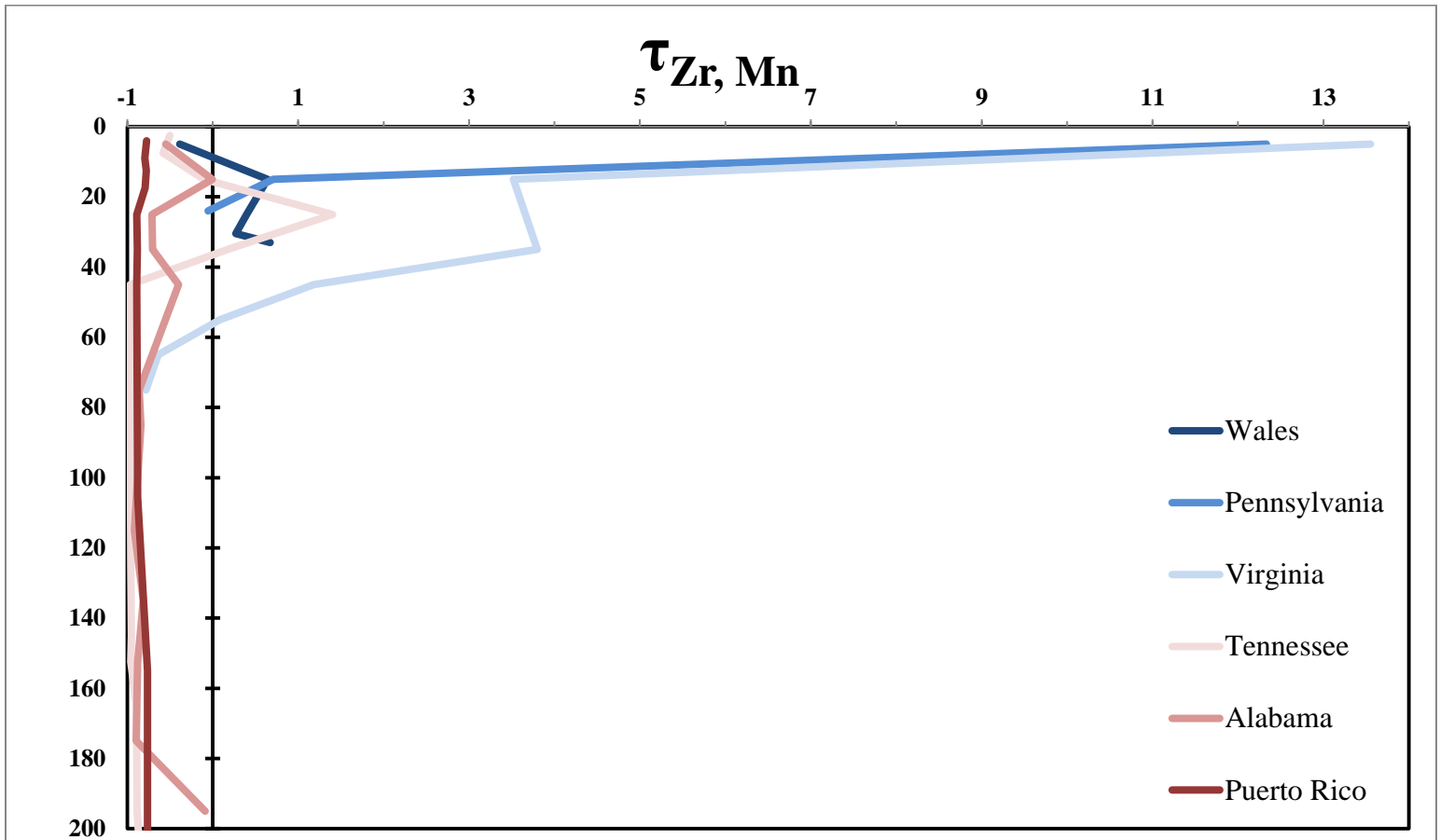


Figure 4. Mass transfer coefficient, τ , for manganese plotted against depth. Parent material is the same parent material used for τ plots of C and N (figures 5 and 6). Zirconium is the immobile element for Wales, PA, TN, AL and PR sites. A corrected titanium concentration was used for the immobile element for VA.

The only sites which show a characteristic addition profile for Mn are Pennsylvania and Virginia. Puerto Rico and Alabama have profiles which are always depleted and relatively constant in the fractional depletion values. Wales becomes enriched at depth, whereas it starts out depleted. Tennessee only shows enrichment between 20 and 40 cm; otherwise the soil is depleted of Mn.

3.3 M_j and m_j trends with MAT

To determine the total C, N and Mn in each profile two different summation methods were used: M_j , which includes the parent material and m_j , which excludes the parent material and accounts for soil strain. These concentration totals will be compared to MAT to determine if

trends exist between the size of our element pools (total concentration for the whole soil profile) and climate.

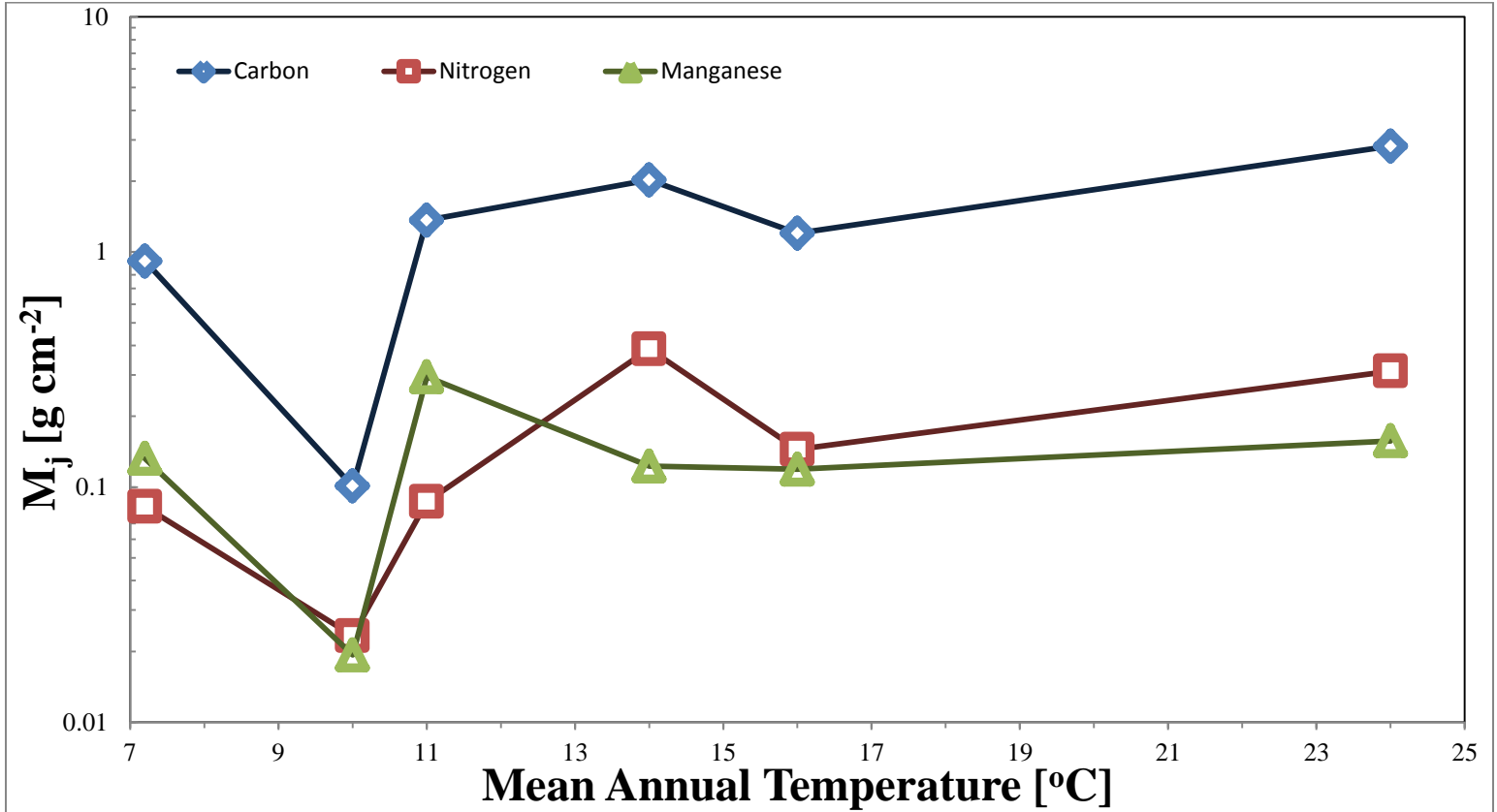


Figure 5. M_j for each element versus mean annual temperature (MAT). M_j is a simple summation of the total concentration in each sample for a soil profile. This total includes input from parent material.

The total concentration of C, N and Mn (M_j) in the soil includes any additions from the parent material. We see that excluding PA there is a general increase in M_j for $j = C, N$ and Mn between Wales and Puerto Rico. Wales and Virginia are the only two sites which show more total Mn than N in the soils. A significant decrease in C, N and Mn concentrations compared to all other sample locations is shown at Pennsylvania.

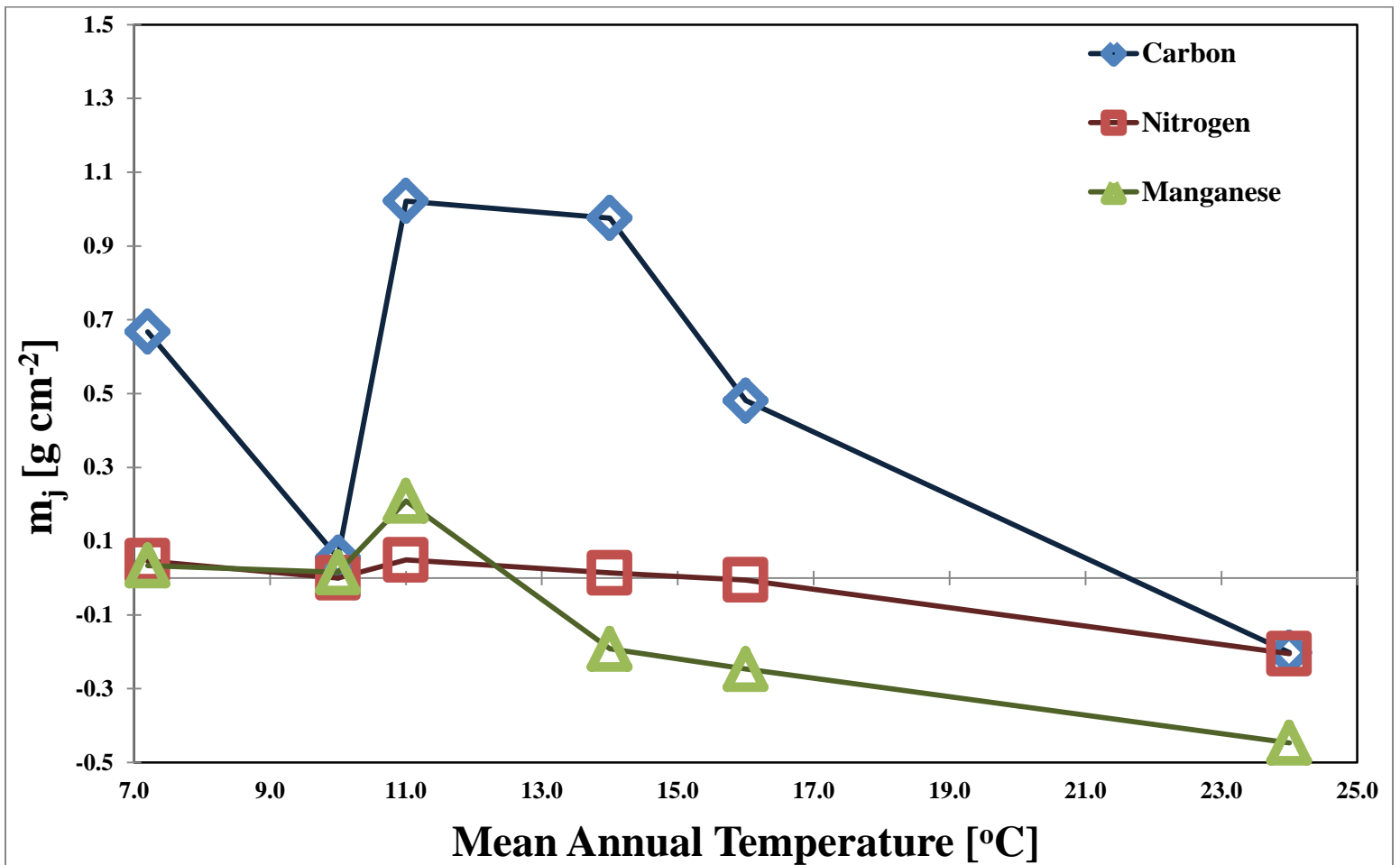


Figure 6. Plots of m_j versus mean annual temperature (MAT). “ m_j ” in this case refers to a summation of element concentrations that excludes input from parent material; it shows net addition or depletion of an element in the soil profile.

The integrated mass flux (m_j) shows the net additions or depletions of a soil profile which have been adjusted for strain. It is hard to see definite trends from our data using this summation style. For all elements, an increasing enrichment to a certain temperature, then a decreasing enrichment to eventual depletion by the warm end-member of the climosequence is observed as a general trend. Pennsylvania is the exception to this trend showing a decrease in total additions from Wales in all elements but especially carbon. Compared to figure 8 which shows Tennessee, Alabama and Puerto Rico with significant accumulations of C, N and Mn, the integrated mass

flux shows a decrease in additions compared to cooler sample locations. The only profile to show all net depletions for C, N and Mn is also the deepest and warmest.

4. Discussion

4.1 C and N coupling in soils

Much of our study is aimed at discovering how and why carbon, nitrogen and manganese are stored in soils in the manners we observed. C/N ratios can tell us how two of our elements change with respect to each other. It is known that the C/N ratio decreases as SOM decomposition increases. Carbon is used in the decomposition process and released from the soil as CO₂ while nitrogen is more likely to be mineralized by organisms and stored in the soil.

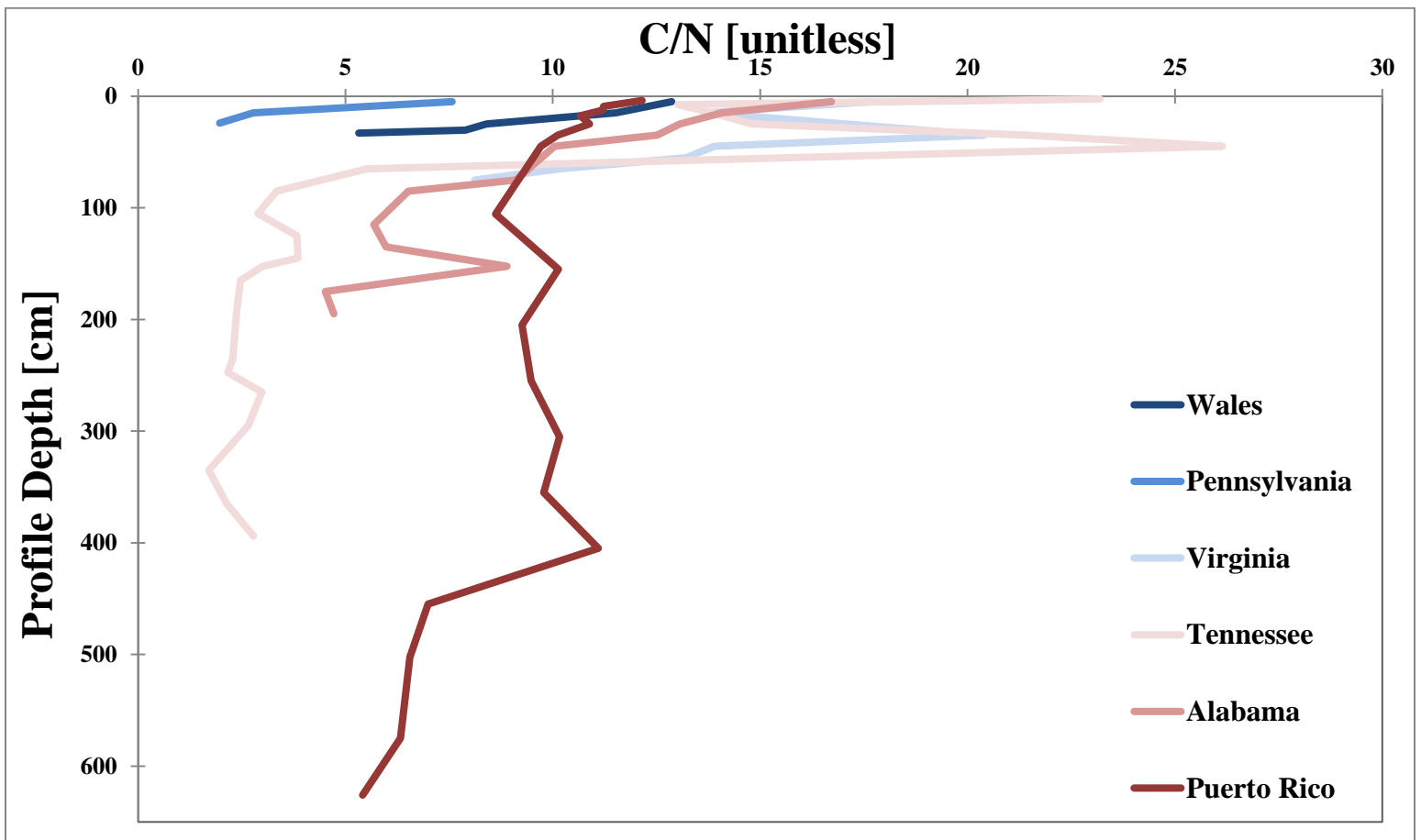


Figure 7. C/N ratio versus depth. C [wt. %] were divided by N [wt. %] and compared against depth. The sample sites are colored to represent the climate gradient (dark blue-coolest to dark red-warmest).

The surface soils for every sample site have the highest C/N ratios. At the VA and TN sites, the C/N ratio increases significantly compared to the rest of the profiles between 30 and 50 cm (C/N=20.39 and C/N=26.14 respectively). At greater depths, the TN profile appears to even out to a ratio of ~4. The VA profile is decreasing similar to the TN profile at greater depths. Wales, PA and AL have generally decreasing C/N ratios with depth. The AL profile does show a small increase in the C/N ratio around 170 cm (C/N=8.89). Puerto Rico has a comparatively steady C/N ratio with depth.

The significant increases of the C/N ratios at the VA and TN sites between 30 and 50 cm depth have two possible causes: SOM translocation and subsequent accumulation deeper in the profile or that new SOM is being introduced via roots at depth. SOM translocation is prevented by increased clay in the soil. The horizon data in figures 21-24 in the appendix shows that the first increased clay layer (Bt horizon) appears right around the same depth that the increases in our element concentrations appear. This would imply that the increased C/N ratios are due to the translocation of SOM from the surface and then the accumulation of SOM at depth via increased clays in the soil at depth. Any small differences in the exact depths at which the Bt horizons first appear and the increases in C appear could be compensated by the fact that the soil samples were not taken per horizon; they were sampled on 10 cm intervals. This means that horizons could be split across sampling intervals and exact concentrations of C, N and Mn per soil horizon would be blurred over depth.

4.2 Model fits

Model equations 8 and 9 based on the Drivas et al. (2011) study were fit to all of our profiles with a range of fit qualities; some fits are better compared to other fits. The equations (8 and 9) were modified by adding the equation to a baseline concentration. This was done because we assumed there was a small background concentration of each element in the soil before the surficial input began. This baseline concentration was assumed to be the parent concentration of

each element in the soil derived from the parent material the soil formed from. The parent concentration of each element in this study was considered the element concentrations in the deepest soil (PA) or an average between the two deepest soil samples (all other sampling locations). These parent concentrations are the same values used to create the τ plots seen in figures 5-7.

The surficial input is used to determine how much C, N or Mn was stored in the soil at after 100 years of deposition. Thus, it does not change the shape of the modeled profile as much as it moves the model fit into a range of concentrations similar to the sampled data. The model underestimates the amount of element input into the soil at the surface because it does not incorporate processes which remove the element from the soil (organic matter decomposition or advection). Thus, the model will require a lower input over time of the element for a given profile then would be predicted if the model included removal terms.

The diffusional mixing coefficient or D_{eff} is the parameter which predominantly creates the shape of the model. This value determines how much the soil is mixed over one year or how much of the surface soil will be moved around to lower in the soil profile. Consequently, the movement of the soil will also transport the surficial input of our elements downward through the profile. A small D_{eff} term ($0-0.5 \text{ cm}^2\text{yr}^{-1}$) would show a large concentration of the element in the surface soils and then a rapid decline to the parent material concentration at depth. Comparatively, a large D_{eff} term would produce a profile that has more of the surficial input distributed at depth. You may still see a high surface concentration but you would also see concentrations much higher than the parent material deeper in the profile.

Large absolute errors which are sometimes observed in the model fits are something that should only be of concern if the model is not following the same general shape of the profile; i.e. the model decreases in concentration with depth in a vertical, linear pattern and then data shows a very large increase in concentration with depth. For the simplicity of the model, if most of the

data points are relatively close to each other (same order of magnitude and under 30% difference between the sample value and the model value) and it is considered a good fit. Often there are large absolute errors between the model and the bottommost sample, which do not necessarily make the model poorly fitting. The profile shape can only take on a few forms when using surficial inputs to keep the modeled concentrations in range with sampled data. Therefore, the modeled profiles shown are objectively good fits for the sampled data.

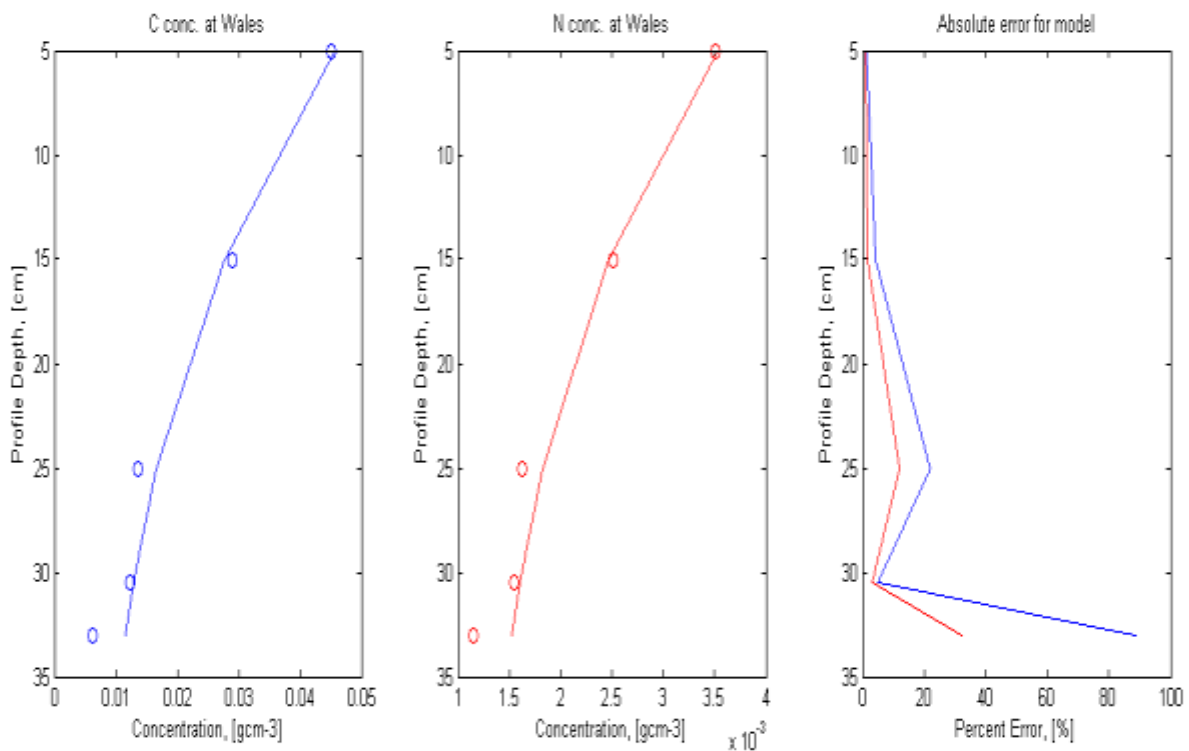


Figure 8. Model fits to carbon and nitrogen concentration in Wales and the absolute error vs. depth for the aforementioned model fits. $Deff = 3.05 \text{ cm}^2 \text{ yr}^{-1}$, C input = $0.008 \text{ g cm}^{-2} \text{ yr}^{-1}$, C baseline = 0.0061 g cm^{-3} , N baseline = 0.0012 g cm^{-3} , N input = $0.000471 \text{ g cm}^{-2} \text{ yr}^{-1}$. Fit was determined best when average absolute error for each profile was minimized while logical conditions were still fulfilled.

The model fits the profiles seen with the exception of the diversion at the lowest sample depth (32.5 cm). The difference between the bottommost sample and the model at this depth is caused by the use of a baseline concentration. The model at this $Deff$ value does not produce values at the baseline concentration at this depth; it is still incorporating element input from the surface at the base of the profile. The particular $Deff$ value was chosen because it provided a good

fit for all the other sampled data higher than the bottommost sample versus other, lower Deff values which increased absolute error significantly at all other data points. There was no reason to try to fit manganese with this model because manganese is depleted at the surface and the model is designed to model addition profiles.

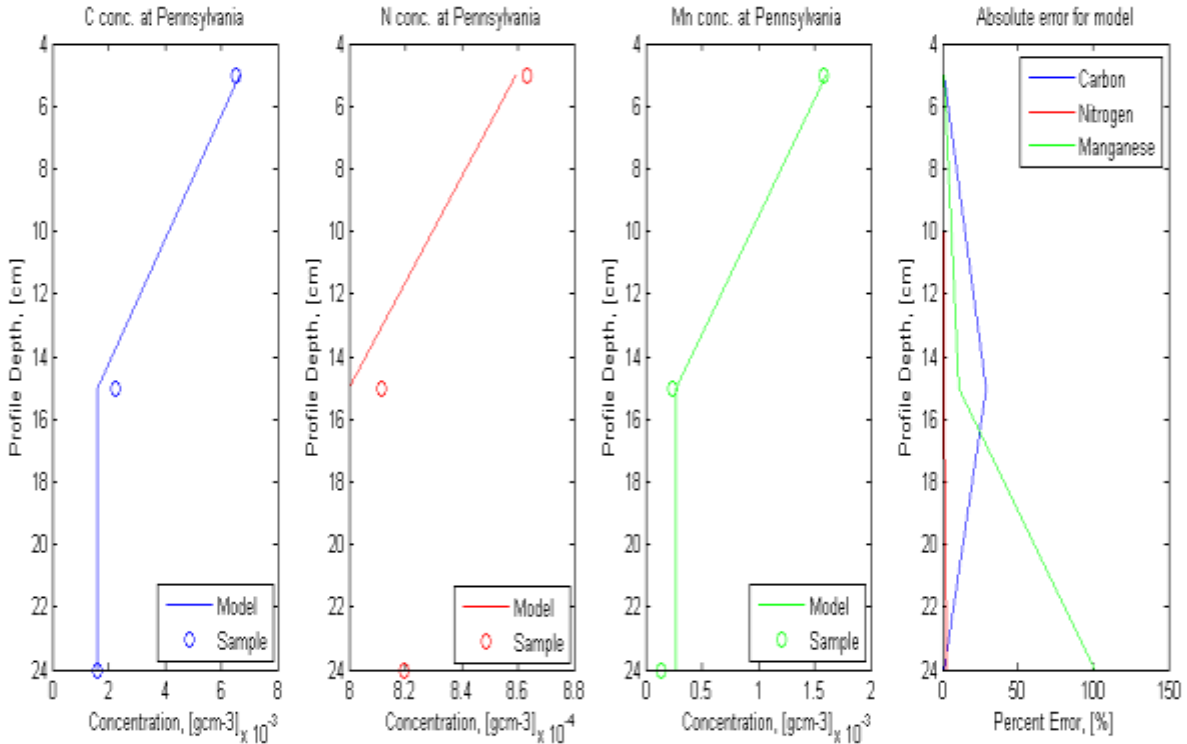


Figure 9. Model fits to carbon, nitrogen, manganese concentration profiles for Pennsylvania and the absolute error vs. depth for the aforementioned model fits. $Deff=0.1 \text{ cm}^2\text{yr}^{-1}$, C input= $0.0085 \text{ gcm}^{-2}\text{yr}^{-1}$, C baseline= 0.0016 gcm^{-3} , N baseline= 0.0008 gcm^{-3} , N input= $0.00001 \text{ gcm}^{-2}\text{yr}^{-1}$, Mn input= $0.00024 \text{ gcm}^{-2}\text{yr}^{-2}$, Mn baseline= $0.000265 \text{ gcm}^{-3}$. Fit was determined best when average absolute error for each profile was minimized while realistic conditions were still fulfilled. Nitrogen is plotting exactly on the $8 \times 10^4 \text{ [gcm}^{-3}]$, thus it is covered by the axis line.

Pennsylvania's soil core showed an addition profile for C, N and Mn (figures 5-7); thus, I used the model to fit all of these elements. In the process of fitting the model, most attention was to the Mn profile fit because the model does encompass Mn transport assuming immobility and in the simplest sense. The increased error at the bottommost sample for Mn does not detract from the quality of the model fit. The concentration produced by the model at the lowest sample

interval was 0.0003 gcm^{-3} and the concentration of the lowest sample is 0.0001 gcm^{-3} . These values are on the same order of magnitude (both 10^{-4}), but the concentration of the model is almost 3 times more than the surface sample. The model is a good fit though because there is no feasible way for the model to fit the top two samples and also the bottom sample.

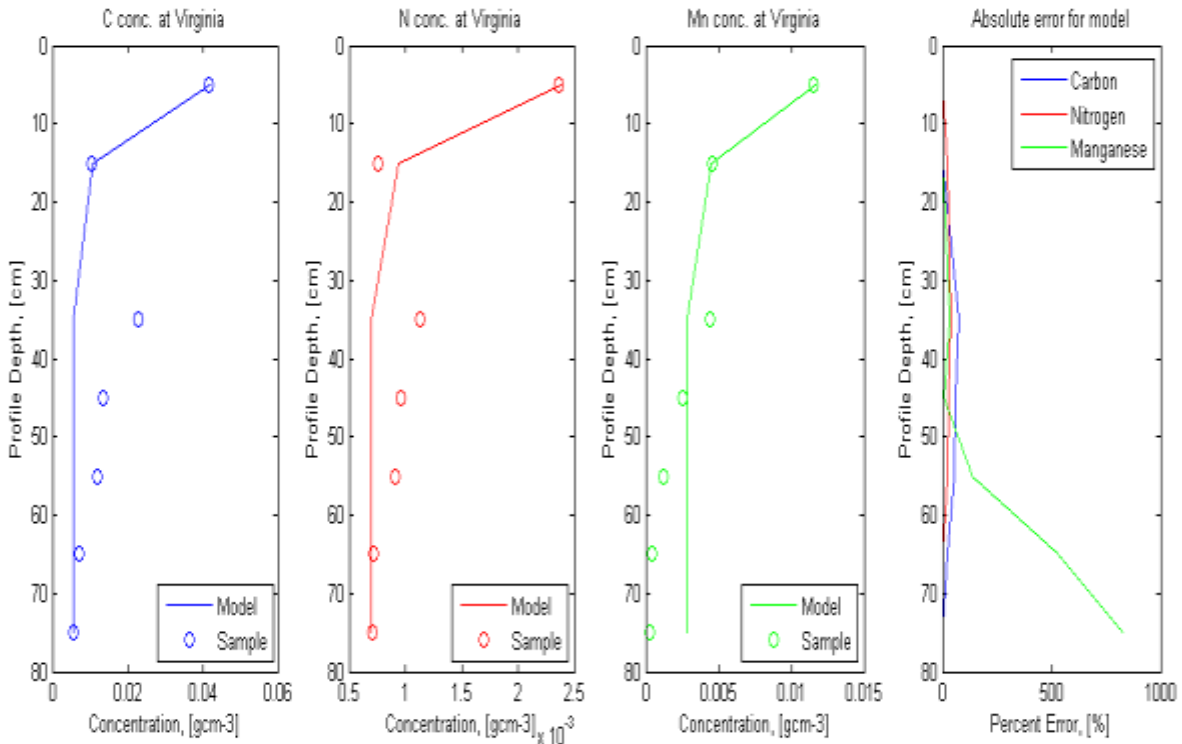


Figure 10. Model fits to carbon, nitrogen, manganese concentration profiles for Virginia and the absolute error vs. depth for the aforementioned model fits. Deff= $0.48 \text{ cm}^2\text{yr}^{-1}$, C input= $0.00457 \text{ gcm}^{-2}\text{yr}^{-1}$, C baseline= 0.0057 gcm^{-3} , N baseline= 0.0007 gcm^{-3} , N input= $0.000212 \text{ gcm}^{-2}\text{yr}^{-1}$, Mn input= $0.00152 \text{ gcm}^{-2}\text{yr}^{-2}$, Mn baseline= $0.000283 \text{ gcm}^{-3}$. Fit was determined best when average absolute error for each profile was minimized while realistic conditions were still fulfilled.

C, N and Mn all showed addition profiles (figures 5-7); thus, the model was run for all of our elements. The model fits for Virginia are poor. The average percent error for C and N are 30.2% and 16.5% respectively, so the fits are technically good for C and N. However, there are basic failings in the model that are noticeable in figure 13. As discussed previously, the C and N concentration profiles have an increase in concentration between 30 and 40 cm (the “bump”). Because of the simplicity of the model, “bumps” such as these are not producible by any means.

Additionally, the Mn profile becomes depleted after 55 cm (figure 7) and once again the model cannot produce depletions of an element due to its simplicity.

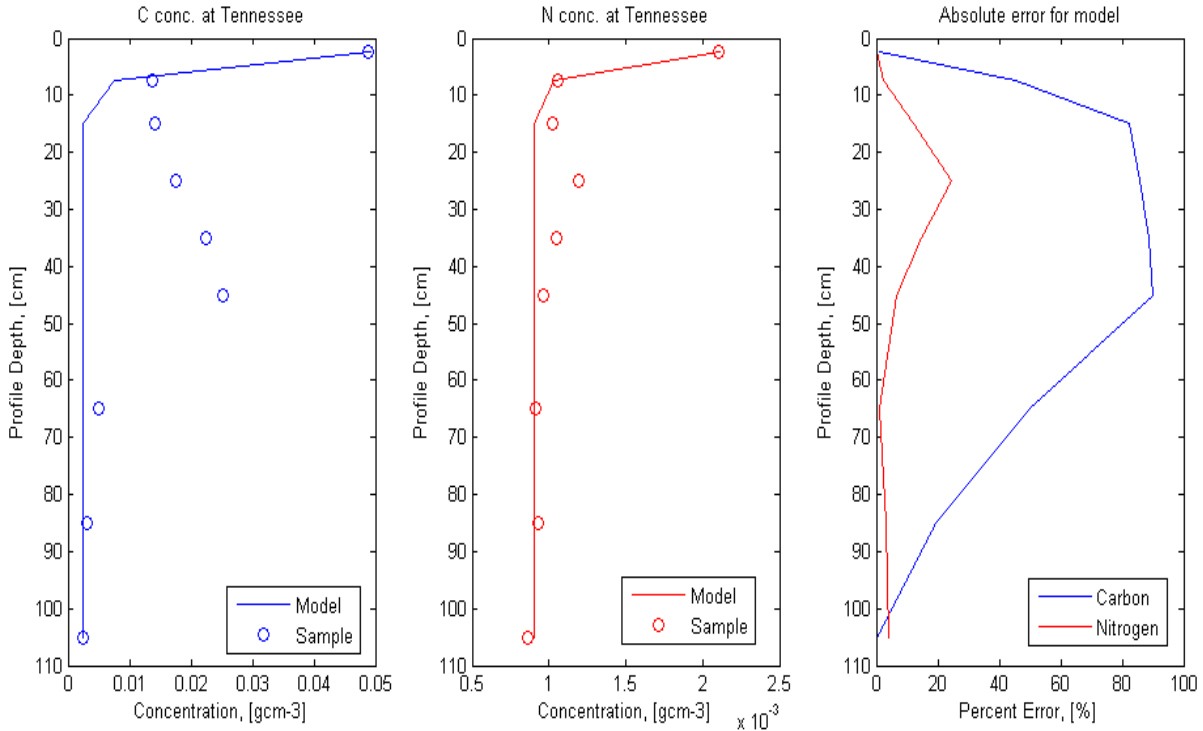


Figure 11. Model fits to carbon and nitrogen concentration in Tennessee and the absolute error vs. depth for the aforementioned model fits. $Deff = 0.1 \text{ cm}^2\text{yr}^{-1}$, C input = $0.0029 \text{ gcm}^{-2}\text{yr}^{-1}$, C baseline = 0.0025 gcm^{-3} , N baseline = 0.0009 gcm^{-3} , N input = $0.000075 \text{ gcm}^{-2}\text{yr}^{-1}$. Fit was determined best when average absolute error for each profile was minimized while logical conditions were still fulfilled.

At the Tennessee sample location, the soil only showed addition profiles for C and N; thus, Mn was not modeled with the Drivas et al. (2011) equation. The fit for TN is also relatively poor due to the increased concentrations observed between 30 and 60 cm (the “bump”). Notice that the absolute error increases in the same range as the “bumps” seen in the C and N concentration profiles. The reason for the failure to fit is the same reason for the VA fit failures; the model is too simple to include processes which would produce concentration increases at depth.

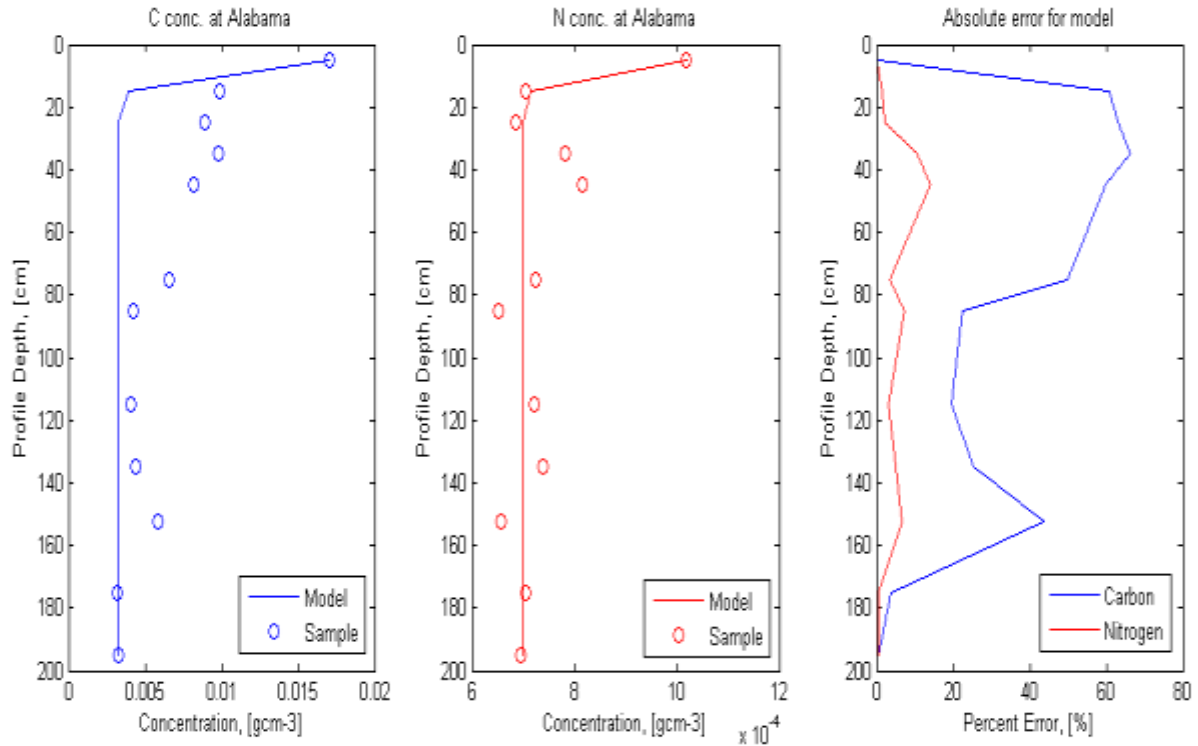


Figure 12. Model fits to carbon and nitrogen concentration in Alabama and the absolute error vs. depth for the aforementioned model fits. $D_{eff} = 0.25 \text{ cm}^2 \text{ yr}^{-1}$, C input = $0.00172 \text{ gcm}^{-2} \text{ yr}^{-1}$, C baseline = 0.0033 gcm^{-3} , N baseline = 0.0007 gcm^{-3} , N input = $0.00004 \text{ gcm}^{-2} \text{ yr}^{-1}$. Fit was determined best when average absolute error for each profile was minimized while logical conditions were still fulfilled.

C and N were once again the only elements to show addition profiles (figures 5 and 6); thus, these were the only two elements modeled using the Drivas et al. (2011) equation at the Alabama sample site. The average absolute error for C was and the average absolute error for N was 34.6 % and 4.5 %. The model fit for AL was moderately poor for C because the model fails to fit the samples' concentrations between 10 and 85 cm when fitting ideally the surface sample and the samples below 85 cm. Once again, there are processes occurring at depth which retains C and the model used does not incorporate processes which would retain C in this manner. However, the average absolute error is low relative to the quality of fit in this case because the fits for half of the samples are very good. Comparatively, the model does a good job at portraying the N concentration profile at Alabama. The fluctuations observed in the profile are small compared to

the concentration values ($\sim 0.00015 \text{ gcm}^{-3}$ compared to $\sim 0.0008 \text{ gcm}^{-3}$). This allows for a very small average absolute error and a good fit.

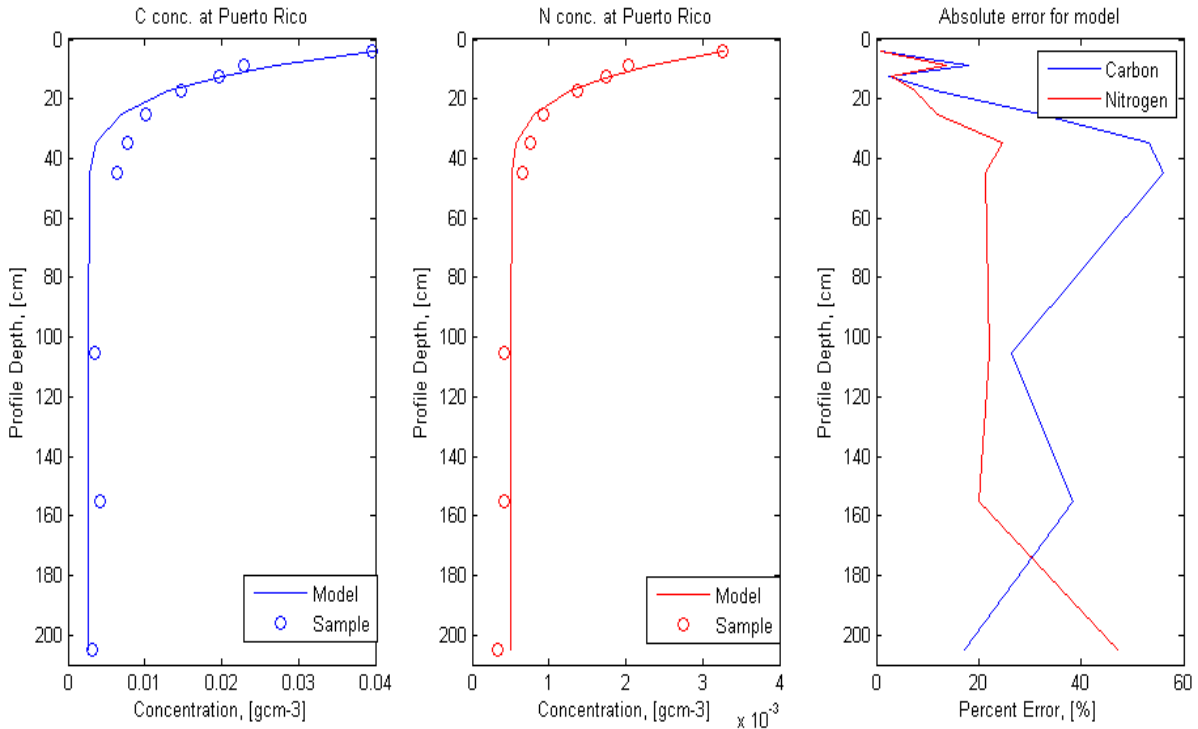


Figure 13. Model fits to carbon and nitrogen concentration in Puerto Rico and the absolute error vs. depth for the aforementioned model fits. $Deff=1.5 \text{ cm}^2\text{yr}^{-1}$, C input= $0.0055 \text{ gcm}^{-2}\text{yr}^{-1}$, C baseline= 0.0026 gcm^{-3} , N baseline= 0.0005 gcm^{-3} , N input= $0.00041 \text{ gcm}^{-2}\text{yr}^{-1}$. Fit was determined best when average absolute error for each profile was minimized while logical conditions were still fulfilled. This model was run using a lower diffusive mixing coefficient. The profile is cropped at 200 cm because the fluctuations in C and N were not significant deeper in the profile.

Puerto Rico presented a challenge when attempting to provide a good fit from the model. C and N were the only elements that showed addition profiles; thus, Mn was excluded from the modeling at this sample location. I present two different good fits for the PR sample site. The first (figure 16) has a lower $Deff$ value. This model was fit by achieving the closest fit for the top three and the lowest three samples in the profile. The resulting $Deff$ value was $1.5 \text{ cm}^2\text{yr}^{-1}$. Figure 17 presents another solution using a much higher $Deff$ value.

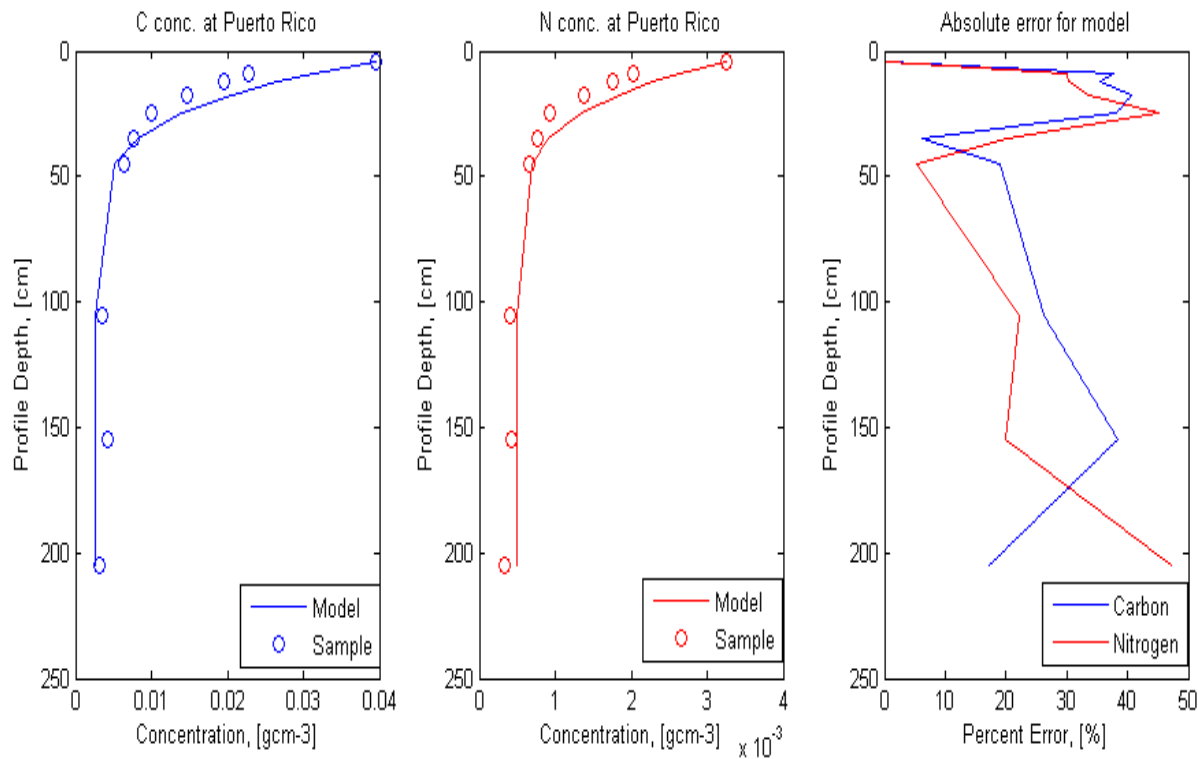


Figure 17. Model fits to carbon and nitrogen concentration in Wales and the absolute error vs. depth for the aforementioned model fits. $Deff= 3.9 \text{ cm}^2\text{yr}^{-1}$, C input=.0078 $\text{gcm}^{-2}\text{yr}^{-1}$, C baseline=.0026 gcm^{-3} , N baseline=.0005 gcm^{-3} , N input=.00058 $\text{gcm}^{-2}\text{yr}^{-1}$. Fit was determined best when average absolute error for each profile was minimized while logical conditions were still fulfilled. This model was run using a higher diffusive mixing coefficient. The profile is cropped at 200 cm because the fluctuations in C and N were not significant deeper in the profile.

The model solution shown in figure 17 determines good fits on the data by minimizing the error between the middle three samples while maintaining a good approximation of the top and lowest three soil samples. This model resulted in a $Deff$ value of $3.9 \text{ cm}^2\text{yr}^{-1}$; a significant increase from the $Deff$ value presented for figure 16. The average absolute error for the C and N fits from figure 16 ($Deff=1.5 \text{ cm}^2\text{yr}^{-1}$) was 25.6% and 17.2% respectively. The average absolute error for the C and N fits from figure 17($Deff=3.9 \text{ cm}^2\text{yr}^{-1}$) was 25.9% and 25.4% respectively. I present two possible good fits for Puerto Rico as it was unclear what depth interval of the profile was most representative of the processes occurring in the soil.

4.3 Climate influence

The goal of our research was to determine first if there were trends with total element pools in the soil when compared against climate (MAT) and then secondly what processes could control the trends we see. From figure 9 we determined that the C and N concentrations increase with increasing MAT to a point (between 11 and 14 °C) and then begin to decrease until eventually all the elements are depleted in the soil with respect to parent material and accounting for soil strain. On a basic level of understanding this could indicate that the rate of input for C and N is increasing at a rate less than the rate of decomposition. The point at which the total pools of the elements begin to decrease with MAT is when the rate of decomposition overtakes any input or storage processes.

While it does not include a decomposition term, the model by Drivas et al does include surficial input rates. If our predictions were accurate from observing trends in figure 9, we should see a general increase in the input of C and N with increasing MAT. Furthermore, I do not expect to see a trend with soil mixing. The processes encompassed in the Deff term can span many climates: frost-wedging, freeze-thaw, bioturbation, root growth (Kaste et al. 2007)

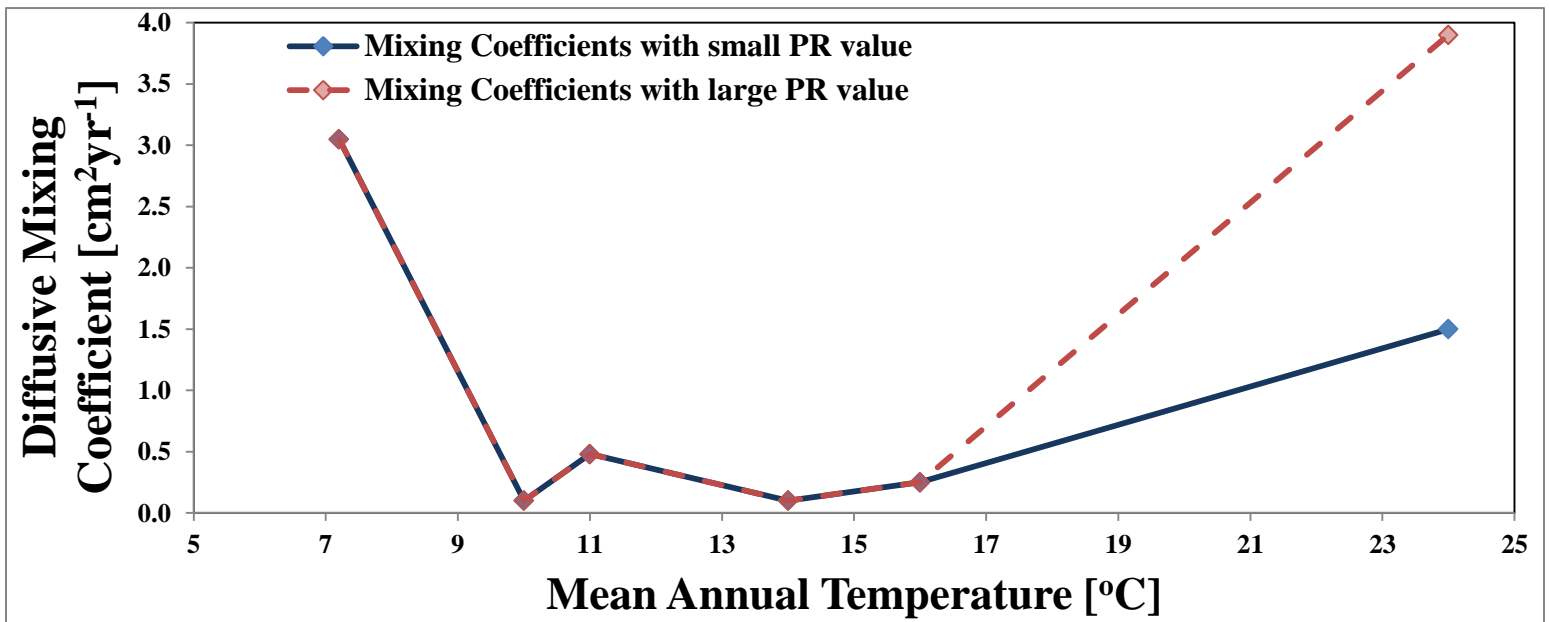


Figure 14. Diffusive Mixing Coefficients vs. Mean Annual Temperature. The “Deff” term from the model which describes how much soil is mixed over a year (diffusive mixing coefficient) was plotted against the mean

annual temperature (MAT) for each sample site. The Deff term was the same for each element modeled per location. The PR location had two model fits which could be ideal with drastically different Deff values. Thus the two different lines plotted in figure 18, one which uses the low Deff value and one which uses the high Deff value.

The higher the concentrations at depth with respect to the parent material, the larger the diffusive mixing coefficient required to fit the data had to be. Thus, Wales and Puerto Rico required a large diffusive mixing coefficient (Deff) values to fit their profiles. These two end members to the climosequence also have one of the most enriched profiles for storage of all elements (W) and the most depleted profile for storage of all elements (PR). Additionally, the other locations were fit with Deff values between 0.1 and 0.48 $\text{cm}^2\text{yr}^{-1}$ and vary arbitrarily with MAT. Because our warmest and coolest sample location have the highest Deff values and the 4 samples sites between them vary arbitrarily with MAT, we can conclude that for our transect the diffusive mixing coefficient does not affect how much C or N is stored in the soil. Subsequently, decomposition of organic matter also is not affected by soil mixing for the soils in this climosequence.

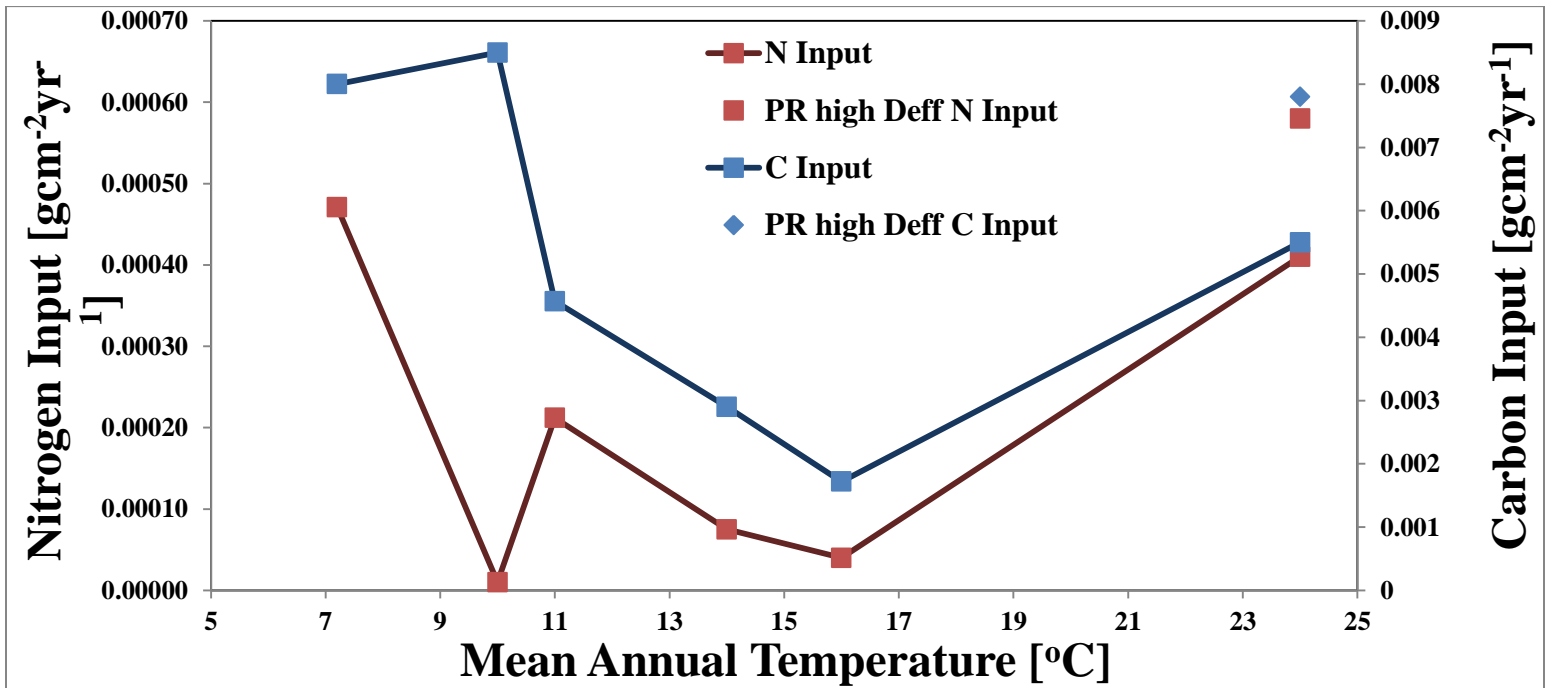


Figure 15. Carbon and Nitrogen inputs derived from the models vs. MAT. Carbon input is plotted against the right axis and nitrogen input is plotted against the left axis. The lone points are the C and N input values for PR when the Deff value is high ($3.9 \text{ cm}^2\text{yr}^{-1}$).

At all sites besides PA, when C increases so does N showing a link between carbon and nitrogen input rates at these sites. Pennsylvania has an increase in C input but a decrease in N input from its surrounding locations, which could indicate an extra source of C in Pennsylvania. Based on total sums of C and N from figures 8 and 9, we would have expected C input to decrease along with the N input decrease. The input of C and N tends to imitate the bowl shape seen in figure 17. The sample sites after Virginia begin to decrease in net additions of the elements until each element is completely depleted in PR (figure 8) and the input values show small decreases at TN and AL, but then large increases at PR (figure 19). This indicates that part of the cause for the decreased total concentrations of C and N in the soils of TN and AL could be attributed to decreased surficial input rates. It also indicates that the most significant effect of decomposition is occurring at Puerto Rico. The input rates are very large compared to the other sites; however, the soil is completely depleted of C and N.

We expected to see an increase in C and N input rates with increasing MAT. On the contrary we see small decreases in C and N input rates at the VA, TN and AL sample sites compared to the three cooler locations. Puerto Rico does however, have an increase input rate of C and N and it is the warmest sample location. It is possible that the small decreases in the C and N input rates at VA, TN and AL sample sites are a product of analysis and that change in MAT ($\sim 5^{\circ}\text{C}$) is not enough to show a clear trend in climate in the soil chemistry. We conclude that decomposition is probably increasing with temperature as evident by the significant depletions of all elements at Puerto Rico despite the high input rates of C and N. Also, the decreased input of C and N at TN and AL sample sites (figure 19) accompanied by the increasing decomposition rate we theorized accounts for the depleting total concentrations seen in figure 9. I suspect that the decomposition rate is not high enough at the VA site and then decrease in C and N input is not enough to show begin to deplete the VA site of C and N. Finally, Mn follows similar trends as C and N in figure 9 (increased total concentration through Virginia and then decreasing total concentration through

Puerto Rico). We only modeled Mn at PA and VA for the sake of model accuracy and sources of additional Mn are almost always point sources such as factories and refineries. Therefore, increases in Mn input rates do not follow a trend with climate. However, Mn can still be weathered out of a soil over time, which is seen in the warmer profiles of this transect (figure 9).

4.4 Error Discussion

4.4.1 Analytical Error

Errors associated with the measured values of C, N and Mn in the soil are small. Reference samples for carbon and nitrogen analysis were measured with a scale of an error of ± 0.005 mg and samples for analyses were measured with a scale of an error of ± 0.05 mg. The CHNS-O Elemental Analyzer included an error of $\pm 0.5\%$ C and $\pm 0.1\%$ for N by reference samples and repeated samples. The limit of detection on the ICP-AES for Mn analysis was 0.005 weight percent and the error is close to $\pm 3\%$ of the recorded value.

4.4.2 Model Error

The model by Drivas et al. is simple in its design which has advantages (fast and easy application to data) but also disadvantages (misses major processes which could be affecting the results). The most egregious error in the model is that C and N are decomposed in soils via microbial action, resulting in a loss of C and N from the soil over time. What this means is that the model will underestimate the surficial input rate of C and N. Precipitation is known to decrease decomposition of organic matter significantly (Jenny 1941). Coupled with very cool mean annual temperatures, the large annual precipitation (table 1) that Wales receives forces the model to portray a more accurate C and N input rate. With minimal decomposition occurring, the model is most accurate for the Wales sample site with regard to C and N model fits and true fit parameter values. These low estimates of C and N input for all the sites excluding Wales could be affecting the trends (or somewhat lack of trends) observed in when comparing input rate to MAT.

Decomposition of organic matter will also alter the shape of the profile; large decomposition rates will decrease the amount of surficial C or N that is found deeper in the profile. The lack of this term may artificially deflate the soil mixing coefficient term (D_{eff}). Thus, some of the soils could have higher D_{eff} values than what the models currently portray. Despite these disadvantages, this model provides a good general picture of what is happening in my soils. I believe that it provides a more accurate picture of Mn than C or N because of the simpler nature of Mn in soils when assuming Mn immobility. This means that the major soil process affecting manganese in soil is soil mixing. To ensure accurate quantification of soil processes to analyze trends with climate, a more complicated model will be necessary.

5. Conclusions

C, N and Mn all have the ability to display addition profiles in soils, indicating net enrichment of these elements compared the parent material and an immobile element in the soil (figures 5-7). These addition profile forming elements can be used to track soil processes and how they fluctuate with climate. The goal of this study was to use the simplest mathematical model possible to analyze how the total concentrations of C, N and Mn changes with climate. We used the previously solved model by Drivas et al. (2011) to fit concentration profiles from a transect of soil sample sites which form a climosequence (figures 11-17). We saw a general increasing enrichment trend in total concentration of C, N and Mn until Virginia ($\sim 11^{\circ}\text{C}$) and then a decreasing enrichment and eventual depletion of all elements by the warmest end member at Puerto Rico (figure 9). The Drivas et al. model allowed us to observe how soil mixing and surficial input varied with climate; these parameters can give us insight into explaining the trends we saw in figure 9. We determined that diffusive soil mixing does not have an effect on the storage of C, N or Mn for our transect. The input rates of C and N form an “up-facing” bowl with increasing MAT, indicating that the input rates of C and N are not the only process which

controls the concentration totals for C, N and Mn in the soil. Additionally, due to the simplistic nature of the model, there is a general under estimate of input rates of C and N. The only case in which C and N input rates may be more accurate is in Wales, where the very large amount of precipitation received annually and the cool MAT retards the decomposition significantly. We believe that decomposition is the process most likely to account for the depletions observed in Puerto Rico and it may play a minor role in the Tennessee and Alabama locations. Overall, the Drivas et al. (2011) model provides a simple and adequate explanation for excess Mn storage and transport in soils but a more complicated model is needed to accurately describe C and N storage and transport in soils.

6. Appendix

Figures 20-26 show the full concentration profiles for C, N and Mn at each sample site along with the field observed profile descriptions (when available). Tennessee is shown with two figures because the profile extends to almost 400 cm, but the physical descriptions for horizons end around 150 cm. Thus, the first profile shows the 0-200 cm and the second shows the full profile 0-398 cm.

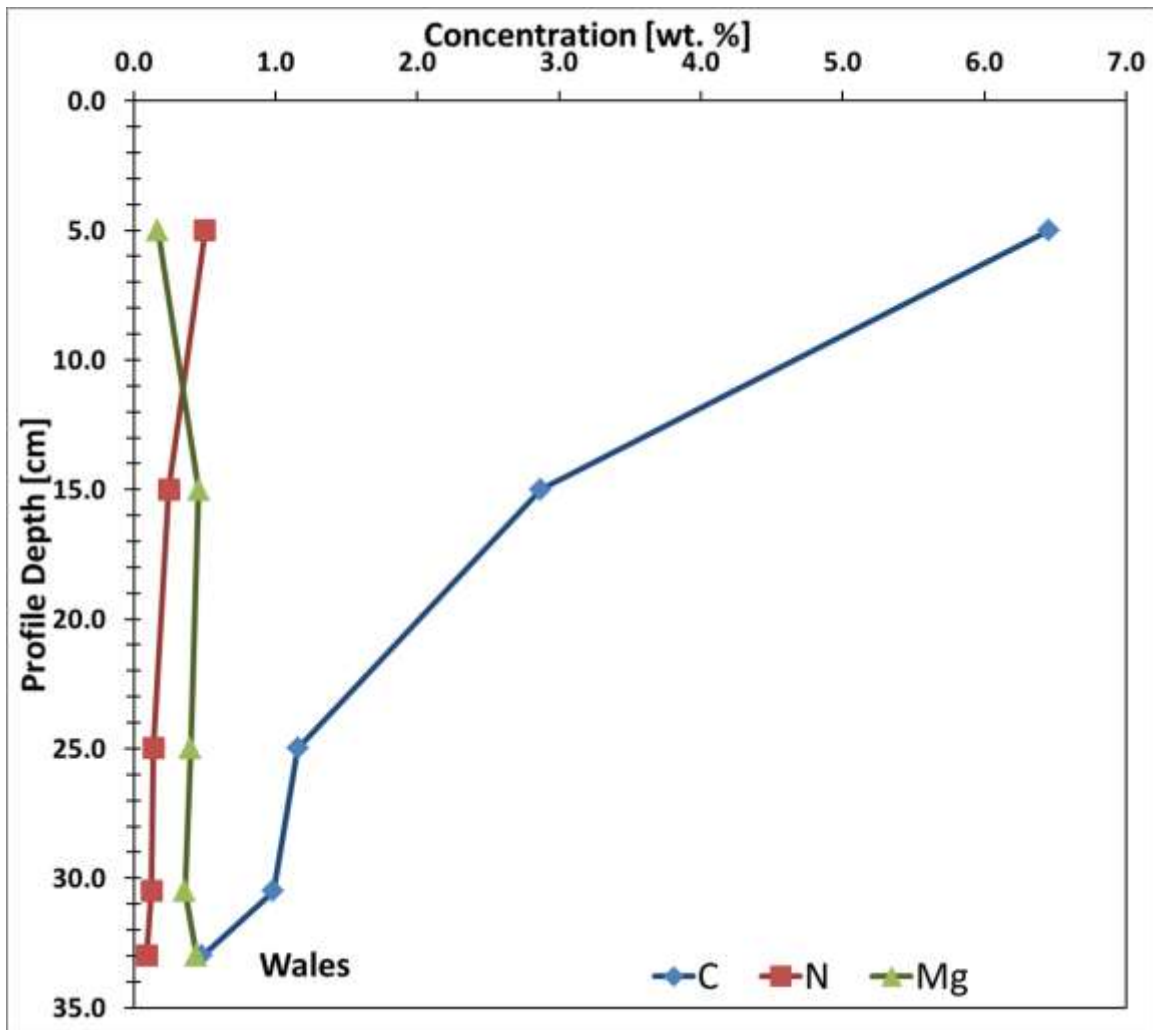


Figure 16. Concentration profiles for Wales.

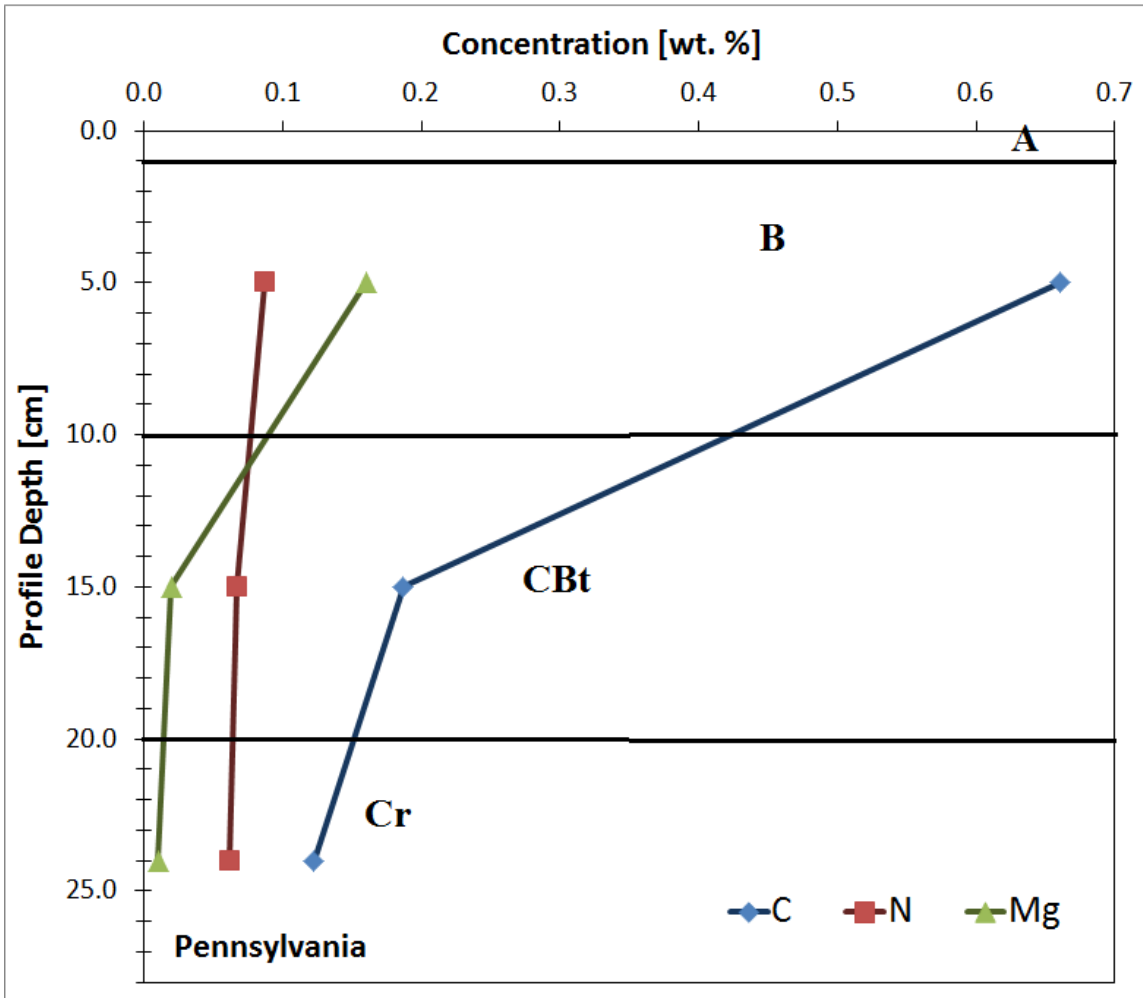


Figure 17. Concentration profiles for Pennsylvania and horizon names.

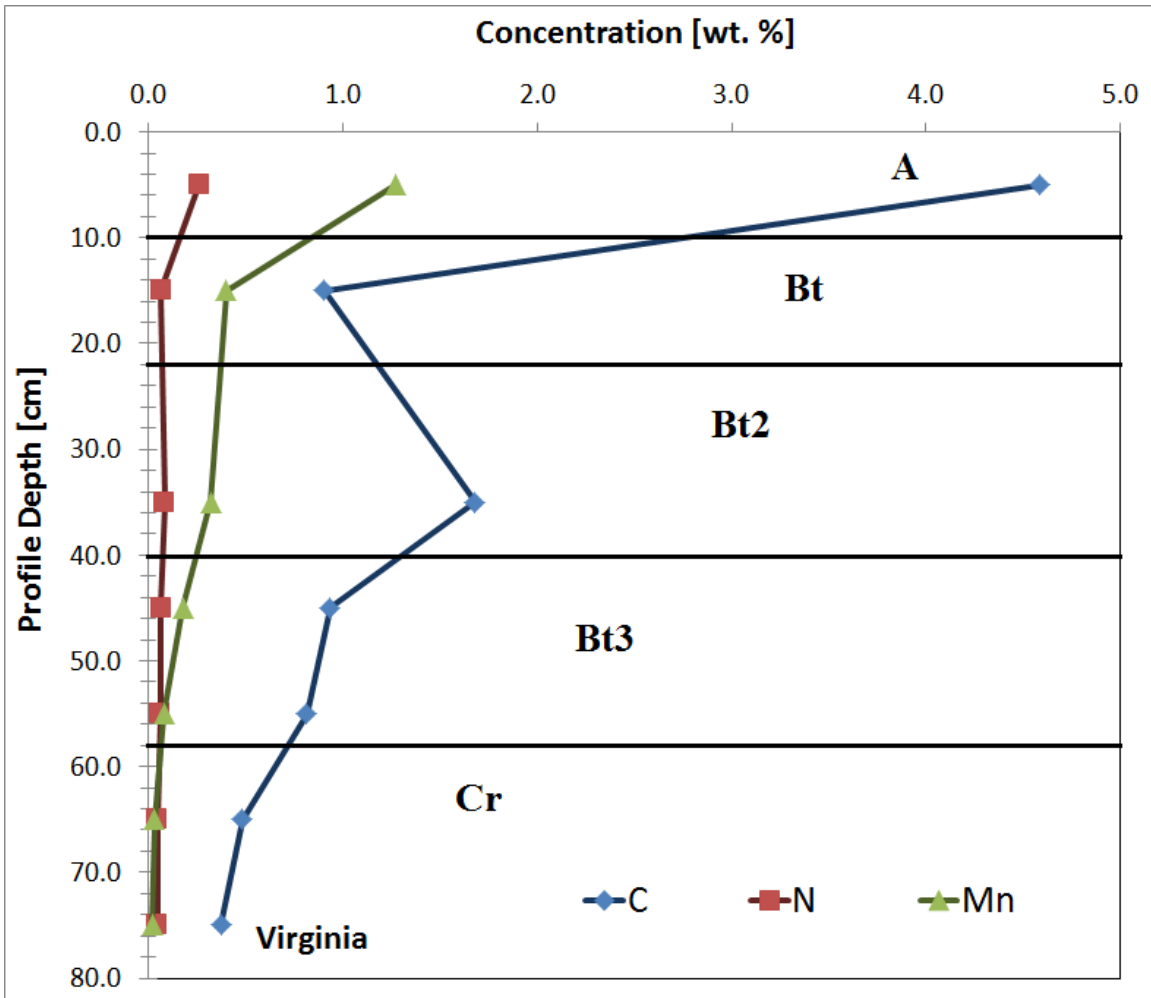


Figure 18. Concentration profiles for Virginia and horizon names.

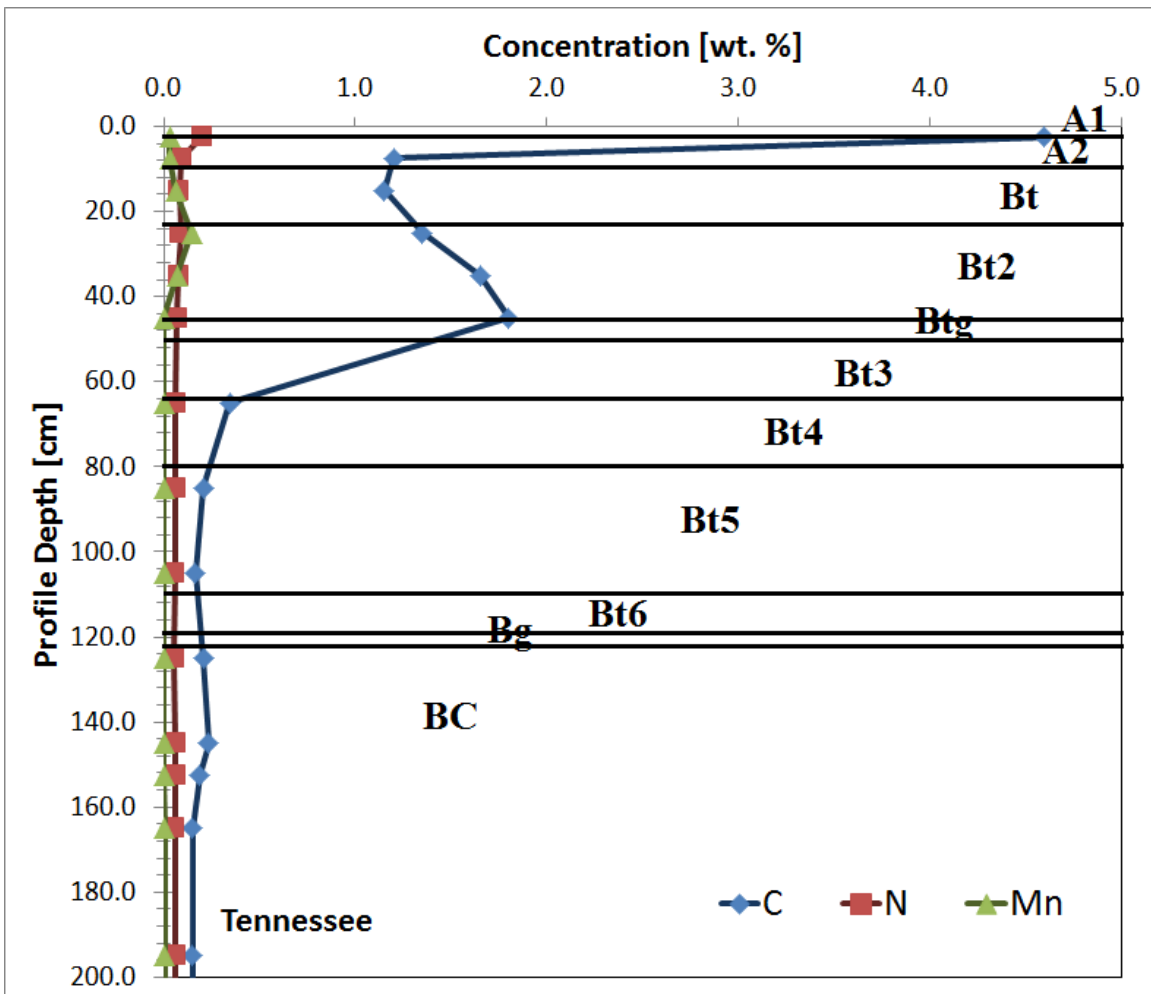


Figure 19. Concentration profiles for Tennessee and horizon descriptions. This profile was abbreviated at 200 cm to show the horizons more clearly.

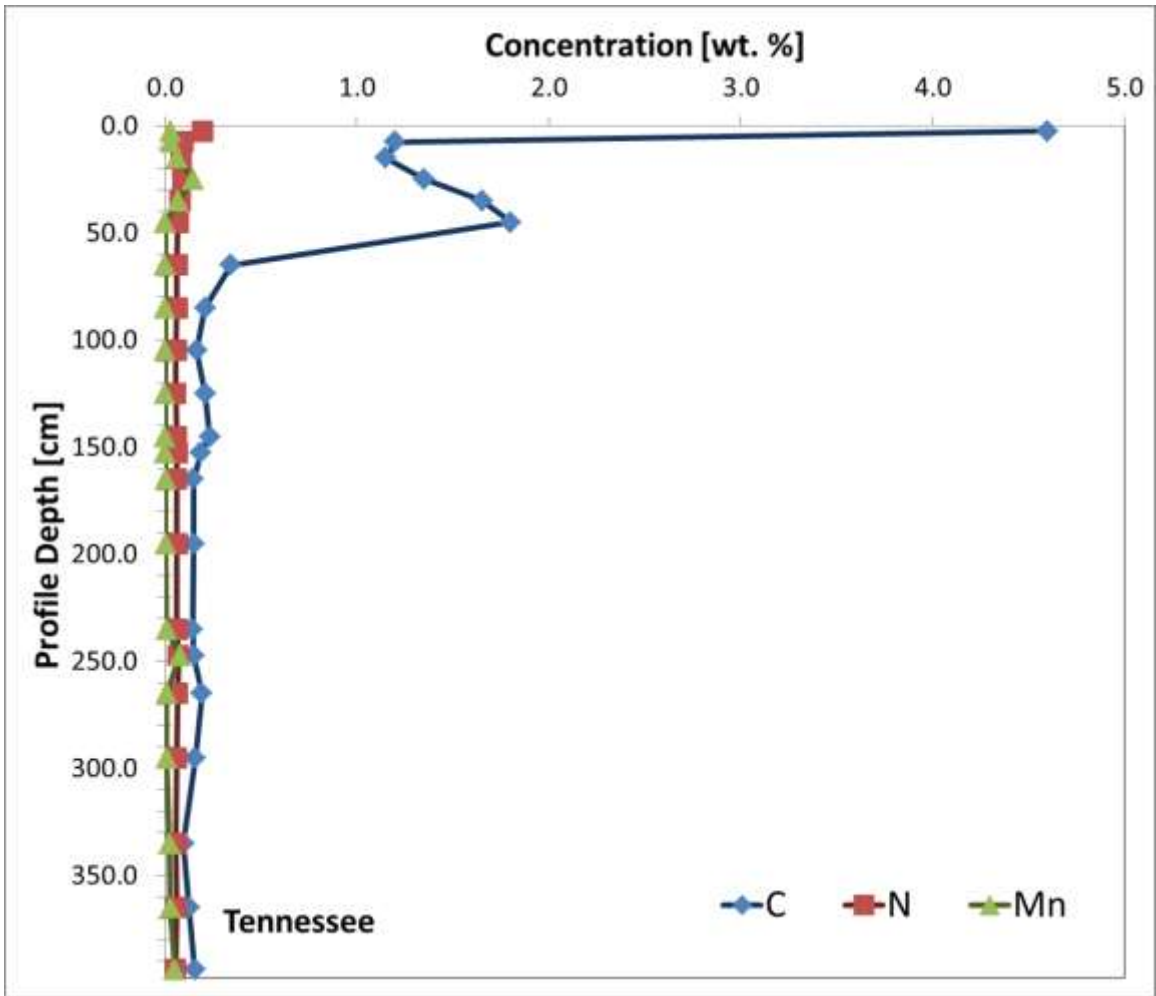


Figure 20. Full concentration profiles for Tennessee.

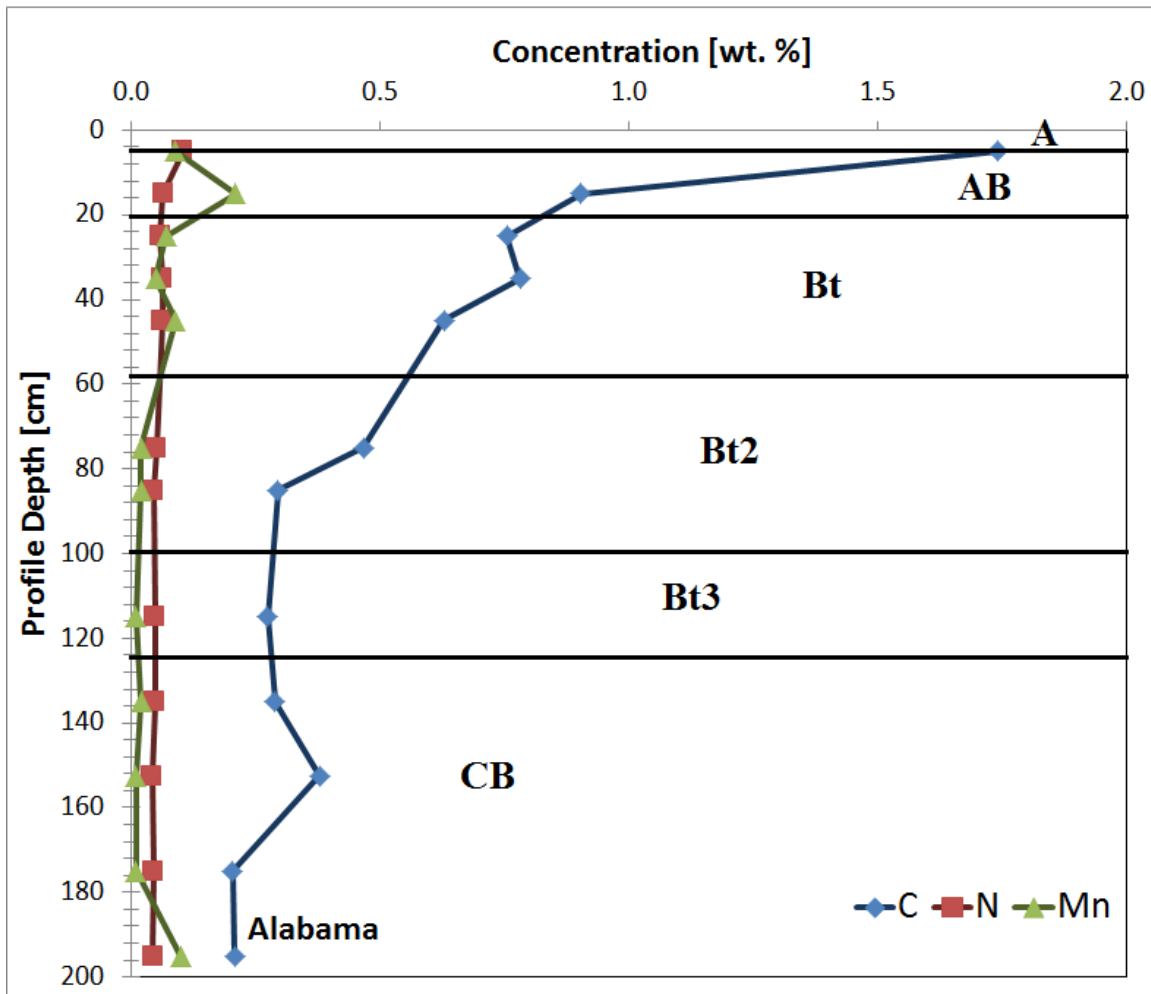


Figure 21. Concentration profiles for Alabama and horizonation.

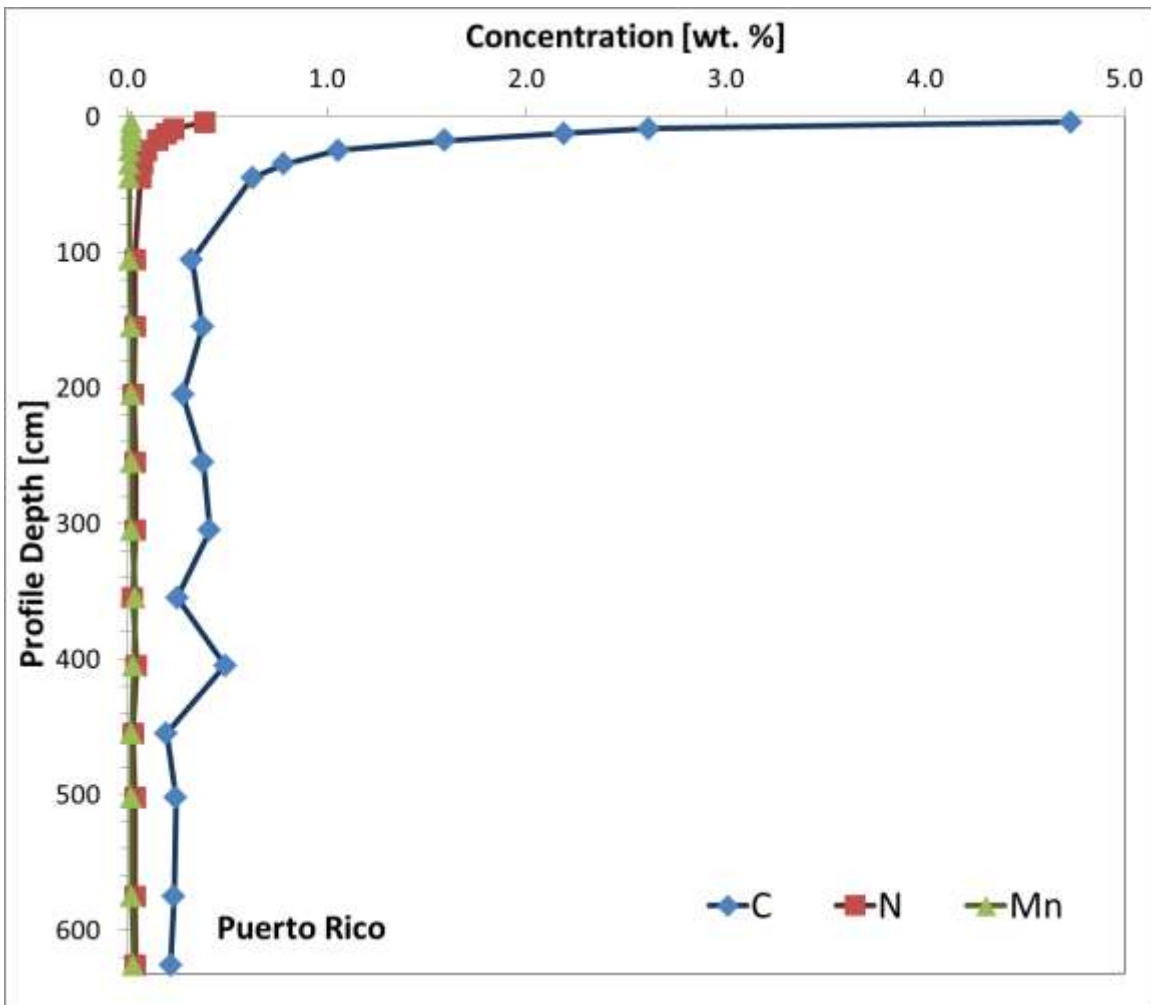


Figure 22. Concentration profiles for Puerto Rico plotted against the full profile depth.

7. Works Cited

- Anderson, Suzanne Prestrud, William E Dietrich, and George H Brimhall Jr. 2002. "Weathering Profiles , Mass-balance Analysis , and Rates of Solute Loss : Linkages Between Weathering and Erosion in a Small , Steep Catchment." *GSA Bulletin* (9): 1143–1158.
- Baisden, W. T., R. Amundson, D. L. Brenner, a. C. Cook, C. Kendall, and J. W. Harden. 2002. "A Multiisotope C and N Modeling Analysis of Soil Organic Matter Turnover and Transport as a Function of Soil Depth in a California Annual Grassland Soil Chronosequence." *Global Biogeochemical Cycles* 16 (4) (December 20): 82–1–82–26. doi:10.1029/2001GB001823. <http://doi.wiley.com/10.1029/2001GB001823>.
- Braakhekke, Maarten C., Christian Beer, Marcel R. Hoosbeek, Markus Reichstein, Bart Kruijt, Marion Schrumppf, and Pavel Kabat. 2011. "SOMPROF: A Vertically Explicit Soil Organic Matter Model." *Ecological Modelling* 222 (10) (May): 1712–1730. doi:10.1016/j.ecolmodel.2011.02.015. <http://linkinghub.elsevier.com/retrieve/pii/S0304380011000962>.
- Brantley, Susan L., and Marina Lebedeva. 2011. "Learning to Read the Chemistry of Regolith to Understand the Critical Zone." *Annual Review of Earth and Planetary Sciences* 39 (1) (May 30): 387–416. doi:10.1146/annurev-earth-040809-152321. <http://www.annualreviews.org/doi/abs/10.1146/annurev-earth-040809-152321>.
- Brimhall, George H, and William E Dietrich. 1987. "Constitutive Mass Balance Relations Between Chemical Composition , Volume , Density , Porosity , and Strain in Metasomatic Hydrochemkai Systems : Results on Weathering and Pedogenesis." *Geochimica Et Cosmochimica Acta* 51 (4).
- Davidson, Erik, and Ivan Janssens. 2006. "Temperature Sensitivity of Soil Carbon Decomposition and Feedbacks to Climate Change." *Nature*.
- Dere, Ashlee L., Timothy S. White, Rich H. April, Brian Reynolds, Thomas E. Miller, Elizabeth P. Knapp, Larry D. McKay, and Susan L. Brantley. 2013. "Climate Dependence of Feldspar Weathering in Shale Soils Along a Latitudinal Gradient." *In Review*.
- Drivas, Peter, Teresa Bowers, and Roberto Yamartino. 2011. "Soil Mixing Depth After Atmospheric Deposition. 1. Model Development and Validation." *Elsevier: Atmospheric Environment*.
- Elzein, Abbas, and Jerome Balesdent. 1995. "Mechanistic Simulation of Vertical Distribution of Carbon Concentrations and Residence Times in Soils." *Soil Science Society of America Journal*.
- Herndon, Elizabeth M, Lixin Jin, and Susan L Brantley. 2011a. "Soils Reveal Widespread Manganese Enrichment from Industrial Inputs." *Environmental Science & Technology* 45 (1) (January 1): 241–7. doi:10.1021/es102001w. <http://www.ncbi.nlm.nih.gov/pubmed/21133425>.

- . 2011b. “Soils Reveal Widespread Manganese Enrichment from Industrial Inputs.” *Environmental Science & Technology* 45 (1) (January 1): 241–7. doi:10.1021/es102001w. <http://www.ncbi.nlm.nih.gov/pubmed/21133425>.
- Herndon, Elizabeth M., and Susan L. Brantley. 2011. “Movement of Manganese Contamination Through the Critical Zone.” *Applied Geochemistry* 26 (June): S40–S43. doi:10.1016/j.apgeochem.2011.03.024. <http://linkinghub.elsevier.com/retrieve/pii/S088329271100103X>.
- Jenny, H. 1941. *Factors of Soil Formation: a System of Quantitative Pedology*. McGraw Hill, NY.
- Jin, L., R. Ravella, B. Ketchum, P. Heaney, and S. Brantley. 2010. “Mineral Weathering and Elemental Transport During Hillslope Evolution at the Susquehanna/Shale Hills Critical Zone Observatory.” *Geochimica Et Cosmochimica Acta* 74: 3669–3691.
- Jobbagy, Estenban G., and Robert B. Jackson. 2000. “The Vertical Distribution of Soil Organic Carbon and Its Relations to Climate and Vegetation.” *Ecological Society of America*.
- Kaste, James M., Arjun M. Heimsath, and Benjamin C. Bostick. 2007. “Short-term Soil Mixing Quantified with Fallout Radionuclides.” *Geology* 35 (3): 243. doi:10.1130/G23355A.1. <http://geology.gsapubs.org/cgi/doi/10.1130/G23355A.1>.
- Medlin, J.H., N.H. Suhr, and J.B. Bodkin. 1969. “Atomic Absorption Analysis of Silicates Employing LiBO₂ Fusion.” *Atomic Absorption Newsletter* 8: 25–29.
- Parton, W.J., M.B. Coughenour, J.M.O. Scurlock, D.S. Ojima, T.G. Gilmanov, R.J. Scholes, D.S. Schimel, et al. 1996. “Global Grassland Ecosystem Modeling: Development and Test of Ecosystem Models for Grassland System.” *SCOPE* 56: 229–266.
- Parton, W.J., M. Hartman, D. Ojima, and D. Schimel. 1998. “DAYCENT and Its Land Surface Submodel.” *Global and Planetary Change* 19 (1-4): 35–48.
- SoilSurveyStaff. 1993. *National Soil Survey Handbook, Title 430-VI*. Washington DC: US Government Printing Office.
- U.S E.P.A. 2003. *Health Effects Support Document for Manganese*. Washington DC.
- Yaalon, D.H., and E. Ganor. 1973. “The Influence of Dust on Soils During the Quaternary.” *Soil Science Society of America Journal*.

ACADEMIC VITA

Nina Bingham

Address: 145 Goddard Circle Pennsylvania Furnace, PA 16865 email:nlb5110@psu.edu

Education

B.S. Geosciences, 2013

The Pennsylvania State University-University Park, PA

Honors and Awards

- Dean's List, George L. Ellis Scholarship (Earth and Mineral Sciences, 2012), the Marathon Oil Scholarship (Earth and Mineral Sciences, 2009-2013), the Teas Scholarship for Excellence (Earth and Mineral Sciences, 2010) and the James and Nancy Hedberg Scholarship in Geosciences (Department of Geosciences, 2011)

Association Memberships/Activities

- GSA, Geological Society of America
- AAPG, American Association of Petroleum Geologists
- SSSA, Soil Science Society of America

Research Interests

I have a broad interest in soil processes and how to model soil processes using mathematical models. Specifically, I am interested in observing trends in element concentrations of a soil as a proxy for how soil processes are acting on a soil.

Professional Presentations

- Research Poster-2012 SSSA Annual Conference at Cincinnati, Ohio
- Research Poster-2013 Carbon Earth Conference at University Park, Pennsylvania
 - 1st place in undergraduate poster competition